DoD EPA DOE

SERDP

Strategic Environmental Research and Development Program

Improving Mission Readiness Through Environmental Research

Development of Innovative Nondestructive Evaluation Technologies for the Inspection of Cracking & Corrosion Under Coatings
SERDP PP-1134

Final Report

Submitted to

Executive Director
SERDP Program Office
901 North Stuart Street, Room 301
Arlington VA 22203-1821

November 2001

Performing Organizations

Naval Surface Warfare Center Carderock Division
Kirsten G. Lipetzky, Code 615
Author of Final Report
Michele Novack, Code 615
Co-PI (Management Lead)
Naval Air Warfare Center Aircraft Division
Dr. Ignacio Perez, Code 4.3.4.2
Co-PI (Technical Lead)

Military Field Activity Partners

Naval Aviation Depot, Jacksonville FL
Warner-Robins Air Logistics Center, Warner-Robins GA
Marine Corps Logistics Base, Albany GA
Naval Aviation Depot, North Island CA

Contractors

Imperium, Inc., Rockville MD
Thermal Wave Imaging, Inc., Detroit MI
Texas Research Institute/ Austin, Inc., Austin TX
Colorado State University, Advanced Microwave Nondestructive Test Lab, Ft. Collins CO
Wayne State University, Institute for Manufacturing Research, Detroit MI

NAVSEA CARDEROCK Surface Warfare Center Division

NAWC Aircraft Division NAVAL AIR WARFARE CENTER

TABLE OF CONTENTS

TABLE OF CONTENTS i

FIGURES iii

TABLES vii

PREFACE viii

PROJECT BACKGROUND 1

EXPECTED PAYOFF 2

OBJECTIVE 2

TECHNICAL APPROACH 3
- **Sample Preparation** 4
- **Real-Time Ultrasound Imaging** 7
- **Thermal Imaging** 7
  - Active thermography 8
  - Sonic thermography 8
- **Near-Field Microwave Imaging** 8

SUMMARY 9
- **Real-Time Ultrasound Imaging** 9
- **Thermal Imaging** 9
- **Near-Field Microwave Imaging** 10

RESULTS AND DISCUSSION 11
- **Real-Time Ultrasound Imaging** 11
  - Through transmission 11
  - Reflection 14
  - Angle beam 17
- **Thermal Imaging** 19
  - Modeling thermal field transient interaction with corrosion pits 20
  - Optimization of the thermographic imaging system 23
  - Active thermography 24
    - Inductive heating 25
    - Laser diode excitation 26
    - Pulse thermography 27
  - Sonic excitation 29
- **Near-Field Microwave Imaging** 30
  - Open-ended coaxial probe 31
  - Open-ended rectangular probe 32

Detection of fatigue cracks 33
Detection of corrosion 38

OTHER PROJECT ACCOMPLISHMENTS 41

CONCLUSIONS 42

TRANSITION PLAN 43

REFERENCES 45

APPENDIX A 47

APPENDIX B 49

APPENDIX C 54

FIGURES

Figure 1. The various types of corrosion that can be found on a typical riveted structure. 4

Figure 2. A typical metallographic image showing exfoliation corrosion of 7075 T6 aluminum. (Cross-sectional view; magnification 100x) 5

Figure 3. Corrosion severity versus number of field in the sample versus time. 6

Figure 4. Percent corrosion (area loss) versus time (seeks) in a salt fog environment for 7075 T6 aluminum sheet. 6

Figure 5. Immersion tank and early through transmission real-time equipment. 12

Figure 6. Through transmission real-time ultrasound image of a composite panel with included flaws showing the detail available at high inspection speed. 12

Figure 7. Through transmission real-time ultrasound image of a plastic millimeter scale. 13

Figure 8. Detection of light corrosion in aluminum 7075 T6 panel. . . . 13

Figure 9. Acoustocam through transmission real-time ultrasound imaging system in C-shaped frame. 14

Figure 10. Schematic drawing of beam splitter reflection camera. . . . 15

Figure 11. Photograph of Acoustocam beam splitter camera. 15

Figure 12. Corrosion pits (1 mm diameter) detected using Acoustocam beam splitter camera viewed from the front surface of the sample through paint. 15

Figure 13. Schematic of re-designed beam splitter reflection camera. . . 16

Figure 14. Honeycomb sample (left) and debonding (right) that has occurred within the sample as detected using the reflection Acoustocam system. 17

Figure 15. Modeling was used to examine the beam inside a plate during one side inspection using the oblique angle reflection method. 17

Figure 16. Schematic of oblique angle reflection camera for real-time ultrasound imaging. 18

Figure 17. Photograph of prototype oblique angle reflection camera. . . 18

Figure 18. Corrosion hidden under paint as imaged with the angle beam reflection camera. 18

Figure 19. Angle beam image of a flat bottom hole showing the multiple images that occur. 19

Figure 20. This figure shows the building blocks of the simple calorimetric model. Two different materials with different density and specific heat comprise the panel. 21

Figure 21. Graph showing the thermal imaging detectability regions in parameter space for two different aluminum panel thicknesses. 22

Figure 22. Aluminum panels with flat bottom holes used to characterize the response of the thermographic system. The panel on the left is 1/8" thick and has 40 flat bottom holes of different radii and depths. The panel on the right is 1/16" thick and has 12 flat bottom holes with much smaller diameters. 23

Figure 23. Thermographic inspection system developed by Thermal Wave Imaging, Inc. 24

Figure 24. Aluminum panel with a fatigue crack in the center. 25

Figure 25. Experimental setup for the inductive heating excitation method of thermal imaging. 25

Figure 26. Thermal contrast generated across the fatigue crack by inductive heating. 26

Figure 27. Experimental setup for laser diode heating excitation method of thermal imaging. 27

Figure 28. Thermal contrast generated across the fatigue crack by laser diode excitation. 27

Figure 29. Schematic diagram of the experimental setup for pulse thermography. 28

Figure 30. The image on the left shows an optical photograph of an F-18 intake panel in which areas of previously detected corrosion have been

ground out. The panel was discolored and had numerous stains. The white areas observed in the thermographic image on the right show regions where corrosion was detected under paint using an optimized pulse thermography system (3 kJ flash energy, 6 0z. uncooled camera, optimized signal processing). 28

Figure 31. Large composite thermographic image of F-18 intake panel created from 8 smaller individual images. 29

Figure 32. Experimental setup for the sonic excitation method of thermal imaging. 30

Figure 33. Thermal contrast generated on the fatigue crack specimen by sonic excitation. 30

Figure 34. (a) Side view and (b) plan view of an open-ended coaxial microwave probe. 31

Figure 35. Schematic of open-ended rectangular waveguide used for detecting fatigue cracks and corrosion under paint. 32

Figure 36a. Crack characteristic signal at 11.3 GHz for a slot with a width of ~0.200 mm and with different depths, coax inner radius of 0.5 mm and outer radius of 1.5 mm. 33

Figure 36b. Crack characteristic signal at 11.3 GHz for a slot with a width of ~0.200 mm and with different depths, coax inner radius of 1.0 mm and outer radius of 4.0 mm. 33

Figure 37. Crack characteristic signal for a fatigue crack with a width of ~3 μm and at a frequency of 11.3 GHz. 34

Figure 38a. Crack characteristic signal for covered crack with one and two layers of tissue paper. 34

Figure 38b. Crack characteristic signal for covered crack with three and four layers of tissue paper. 35

Figure 39. Influence of frequency and incident power on covered crack detection for a slot with a width of 0.15 mm and a depth of 0.75 mm and coating (tape) thickness of 0.11 mm. 35

Figure 40a. Higher order mode signal generated by the open-ended rectangular waveguide probe for an exposed crack with a width of ~0.1 mm and a depth of 0.9 mm. 37

Figure 40b. Higher order mode signal generated by the open-ended rectangular waveguide probe for a covered crack with a coating thickness of 0.05 mm and crack width of ~0.1 mm and a depth of 0.9 mm. 37

Figure 40c. Higher order mode signal generated by the open-ended rectangular waveguide probe for a covered crack with a coating thickness of 0.15 mm and crack width of ~0.1 mm and a depth of 0.9 mm. 37

Figure 41. Sample plates C (left) and B (right) showing corrosion before being painted, with areas scanned highlighted. 38

Figure 42. Image acquired using an open-ended rectangular waveguide probe of the top-middle strip of the front of panel B, at a frequency of 24.1 GHz and at a standoff distance of 0 mm (i.e. in contact). (Note: Dimensions are in mm). 39

Figure 43. Image acquired using an open-ended rectangular waveguide probe of the top-middle strip of the front of panel B, at a frequency of 24.1 GHz and at a standoff distance of 5 mm. (Note: Dimensions are in mm). . 40

Figure 44. Image acquired using an open-ended rectangular waveguide probe of the top strip of the front of panel C, at a frequency of 24.1 GHz and at a standoff distance of 5 mm. (Note: Dimensions are in mm). . . 40

Figure 45. Image acquired using an open-ended rectangular waveguide probe of the middle strip of the front of panel C, at a frequency of 33.5 GHz and at a standoff distance of 2 mm. (Note: Dimensions are in mm). . 40

Figure 46. Image acquired using an open-ended rectangular waveguide probe of the top-middle strip of the front of panel C, at a frequency range of 33.5 GHz and at a standoff distance of 2 mm. (Note: Dimensions are in mm). 41

TABLES

Table 1. Corrosion, fatigue, and various manufactured samples. . . . 5

Table 2. Comparison of all the thermal imaging techniques studied under the SERDP program. 10

PREFACE

This document was written as a compilation of work performed under the SERDP sponsored program “Innovative Technologies for the Inspection of Cracking and Corrosion Under Coatings” (PP-1134) over the two year period FY99-FY00. Every endeavor has been made to incorporate all materials associated with the project including Annual Reports for FY99 and FY00, presentations, technical papers, electronic files and documents, and personal communications.

Kirsten G. Lipetzky, Ph.D.

PROJECT BACKGROUND

This project responded to the well documented, tri-service need for NDE technology to both support condition-based maintenance programs for military assets and, more importantly, minimize or mitigate the various streams of VOC and HAP pollutants and other hazardous wastes which create significant environmental compliance burdens for DOD. These basic issues are faced by other federal agencies as well as commercial industries, but the sheer volume of ferrous and non-ferrous metallic weapon platforms and military infrastructure has always presented a formidable life-cycle management problem due to the ever-present natural tendency for metals to degrade in the operating environment.

Conventionally, the problems of corrosion (chemical degradation) and fatigue cracking (mechanical degradation) have been addressed with the use of surface coatings (e.g. organic solvent-based paints) and periodic NDE inspections (e.g. eddy current or magnetic particle methods). These practices have evolved over the years with the introduction of technologies offering better performance, but they always remained a significant portion of the maintenance budget for each system and played a major factor in overall system readiness especially since conventional NDE methods have required the removal of surface coatings in order to effectively conduct interrogations of the metallic substrate. With the dawn of environmental compliance mandates, attention has focused on the significant volume of air pollutants and hazardous waste by-products generated by aircraft, ground vehicle, and even shipboard maintenance practices. The disposal costs for these wastes is in the millions of dollars and is increasing.

In July 1997, the SERDP Coatings & Coatings Removal Workshop reviewed the Joint-Service user requirements and formulated the following *high priority* needs:

- “NDE of Paint and Corrosion Under Paint” - techniques needed to determine the extent of corrosion damage to aluminum structure beneath coatings systems without requiring the removal of the coating.

- “Pre-Evaluation Technique/Process to Determine if a Coating Needs to be Removed” - coatings are often stripped from weapons systems in order to evaluate the substrate characteristics, not because of poor coating performance. Capability to inspect “through the coating” would decrease the frequency the number of stripping and repainting cycles.

In addition, the Joint Air Force/FAA/NASA Aging Aircraft Plan, has noted the following similar need:

- Improved non-visual techniques for finding hidden corrosion using a variety of techniques. Must have the capability to discover and roughly quantify hidden

corrosion without requiring disassembly of the aircraft. (20% of all needs relating to aging aircraft are for corrosion detection. As a result, new methods of NDE for hidden corrosion are the #2 strategic priority of the Aging Aircraft Plan. "Green" coating systems are the #1 priority)

These needs also tie-in with the FY98 Defense Technology Area Plan, Defense Technology Objective (DTO) MP.07.01—Material and Processes for Metal Cleaning, Corrosion Control, and Coatings. This DTO is from the Civil Engineering & Environmental Quality Sub-area, Pollution Prevention Sub-Sub-area. The objective is to research and develop innovative technologies for preventing pollution while maintaining warfighting capabilities. Current efforts focus on the development of "green" paints, coatings, surface preparations and treatments, and the associated enabling technologies. The February '98 TARA briefing identified *early corrosion detection capability as a "hot need" and nondestructive analytical techniques as the respective new thrust area.* According to the presenters at the briefing, *"the ability to detect and repair corrosion areas prior to severe degradation will improve operational readiness and reduce operational maintenance cost by 25%."*

EXPECTED PAYOFF

Reduced frequency of depaint/paint operations leading to significant cost savings, reduced environmental pollution, and enhanced operational availability. Economic benefits will result by reducing the amount of work required to continually strip/repaint, and aircraft would be more available for field operations, thus enhancing force readiness. "Inspection-through-paint" is a prerequisite for long coating system life, and selective stripping of topcoats without removal of corrosion protection layers and the achievement of true condition-based maintenance.

OBJECTIVE

The objective of this program was to develop and evaluate three innovative technologies for their viability as nondestructive evaluation tools for the detection of cracks and corrosion under surface coatings in aircraft and ground vehicle applications. They had been developed in the private sector under either private or Navy SBIR program funding and had shown promise for meeting the technical and sometimes unique logistical needs of DOD aircraft and ground vehicle applications. The technologies included:

- Ultrasound Imaging (Imperium, Inc.)
- Thermal Imaging (Thermal Wave Imaging, Inc. and Wayne State University/Institute for Manufacturing Research)

- Near-Field Microwave Imaging (Texas Research Institute/Austin and Colorado State University/Advanced Microwave Nondestructive Test Lab)

In particular, these technologies were selected for their potential to inspect areas rather than points (translating into efficient levels of inspection scan rates), portability to the job site, overall projected economy to implement, and relative technological maturity. For example, the feasibility of using microwaves to locate hidden corrosion under shipboard paint had already been demonstrated under a Navy contract, however, the technology was in need of transition funding to build prototypes for a commercial hardware offering. Microwave detection of cracks under paint on steel substrates had been addressed in the university environment, and was ready to transition to practice. The head start advantage of this technology did not mean it was without risk, but it also meant that a product with positive environmental impact could be produced in the SERDP time frame if the risks were overcome.

While not always apparent, there was a sense of urgency for addressing this SERDP need. Goals were in place to *reduce paint stripping and application toxic waste by 50% by FY2001.* And, as in most research in support of pollution prevention, the economic incentives were reductions in operational and environmental compliance costs, disposal costs, workplace exposures to hazardous materials, and long-term liabilities and clean-up costs.

TECHNICAL APPROACH

No matter how good a coating system is, over time it will degrade and the corrosive environment will leak in. This is especially true in aircraft structures where, due to fatigue, UV radiation, and high loads, the coating embrittles. Accelerated fatigue develops predominantly around high flex area at joints and around rivets. In Figure 1 cracks are shown developing around rivets and along a butt joint. Once a crack is formed in the coating, the environment will leach in and corrosion will start to develop. Depending on the material, coating, location, and structure, different types of corrosion will develop such as pitting corrosion, exfoliation, filiform, crevice, and third layer. Most of the effects of corrosion remain hidden from the naked eye until the damage is so significant that the entire structure is placed in danger and major overhaul of the structure is required. Corrosion substantially reduces the strength of materials either by thinning the material, by plastically deforming the materials due to accumulation of debris or by introducing stress raisers. In every case the strength of the structure is significantly reduced. Early detection and quantification of corrosion without removing the paint system can significantly enhance the life of these structures while minimizing the environmental impact.

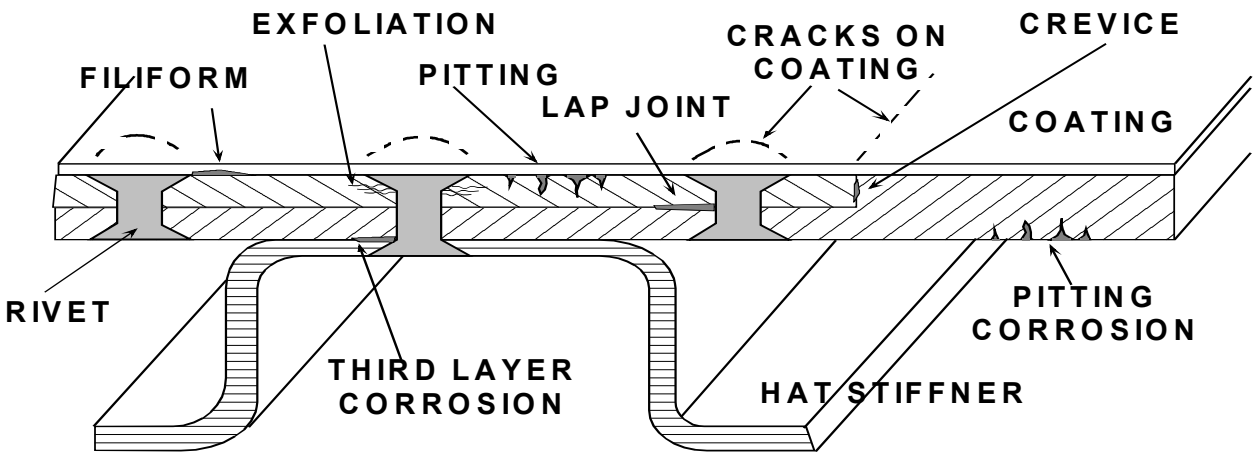

Figure 1. The various types of corrosion that can be found on a typical riveted structure.

In order to properly detect corrosion and diagnose the severity and the impact that it might have on the structure, advanced nondestructive evaluation (NDE) methods are required as well as corrosion models that correlate the NDE signal with the severity of corrosion. In this program three NDE techniques for the detection of corrosion were evaluated, namely Ultrasound Imaging, Thermal Imaging, and Near-Field Microwave Scanning. These techniques were also believed to be effective in detecting cracks under coatings and were investigated for that purpose as well. In a parallel effort to NDE technique development, models were developed to correlate with the output signature of the various techniques.

Sample Preparation

Corrosion, fatigue, and other manufactured samples were fabricated from aluminum alloy 7075 T6 plate. Alloy 7075 T6 was selected based on the fact that it is a common alloy used in the aircraft industry and was also known to corrode fairly rapidly (a benefit when producing artificially corroded samples). A list of the types of samples that were manufactured appears in Table 1.

A salt fog environment was used to induce corrosion in some of the plates manufactured for this study. The degree of corrosion could be controlled by the duration of the exposure of a plate to the salt fog environment. In addition, it was possible to restrict the corrosion to certain areas on a plate by protecting the majority of a given sample with MIL-P-85582 primer (waterborne, Type 1 Class C—a chromate primer) and MIL-PRF-85285 topcoat (aviation gray paint) and leaving the remaining portion of the sample uncoated and susceptible to the salt fog environment.

The corrosion rate of the samples was studied by metallographically examining the samples that had been corroded in the salt fog environmental chamber for various time periods. The area of each corrosion pit was measured and recorded utilizing a computer based metallographic image analysis system. A

Table 1. Corrosion, Fatigue, and Various Manufactured Samples

Corrosion Samples
✡ Set 1 - Heavy corrosion, salt fog plus SO_2 (all paint came off)
✡ Set 2 - Light corrosion, salt fog (paint still on samples)
✡ Set 3 - Bare panels without protection
Manufactured Samples
✡ Crack Samples
✡ **F1-F4** Fatigue cracks approx. 1" long in 0.062 plate
✡ Flat Bottom Holes (FBH)
✡ **A1** 2" x 4" x 1/16" plate, 0.187" diameter hole 0.005"/0.007" deep inside/outside
✡ **A2** 3" x 3 3/4" x 1/16" plate, 0.187" diameter hole 0.012"/0.012" deep inside/outside
✡ **A3** 2 3/4" x 4" x 1/8" plate, 0.187" diameter hole 0.01"/0.025" deep inside/outside
✡ Painted Samples
✡ **P1** 5 1/2" x 7 1/2" x 1/8" plate, 20 each 0.03" diameter holes 0.01"/0.05" deep under 0,2,4, and 6 mils of paint
✡ **P2** 5 1/2" x 7 1/2" x 1/16" plate, 20 each 0.03" diameter holes 0.01"/0.05" deep under 0,2,4, and 6 mils of paint
✡ Plug Specimens
✡ Welded Specimens

typical metallographic image is shown in Figure 2. The quantitative study of corrosion rates yielded information about both pit formation and overall corrosion rate. Figure 3 provides a graphical presentation of the size and number of pits observed as a function of exposure time in the salt fog environment. Initially the corrosion pits were small and scattered evenly about a given sample. (See the four-week exposure distribution in Figure 3.) As the exposure time increased there was no increase in the distribution of the small pits but an increase was observed in the number of large pits. (See the seven-week exposure distribution in Figure 3). Advanced corrosion regions contained pits on the order of 0.020 inch diameter and larger.

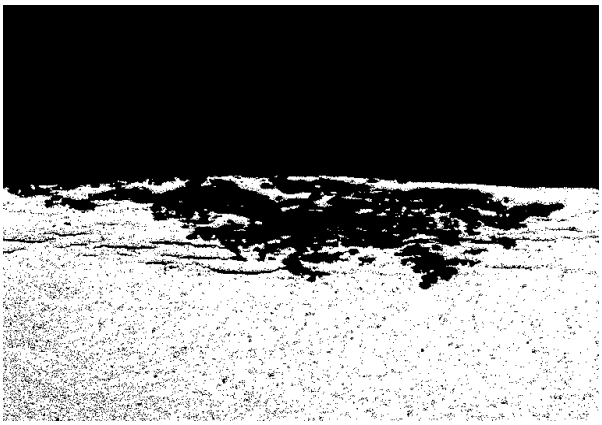

Figure 2. A typical metallographic image showing exfoliation corrosion of 7075 T6 aluminum. (Cross-sectional view; magnification 100x)

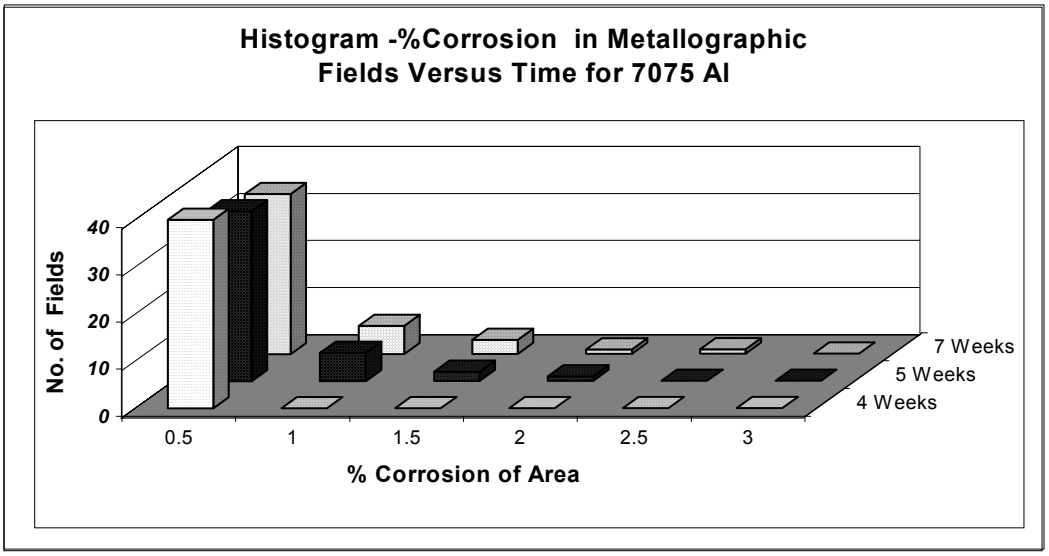

Figure 3. Corrosion severity versus number of fields in the sample versus time.

The study of the growth rate of the pits with regard to mean, average, and maximum value clearly demonstrated the formation of small numbers of larger pits as time progressed. The average corrosion severity (% area loss), as calculated, increased only slowly while the maximum corrosion severity increased at a much greater rate as the smaller number of pits grew rapidly. See Figure 4 for clarification.

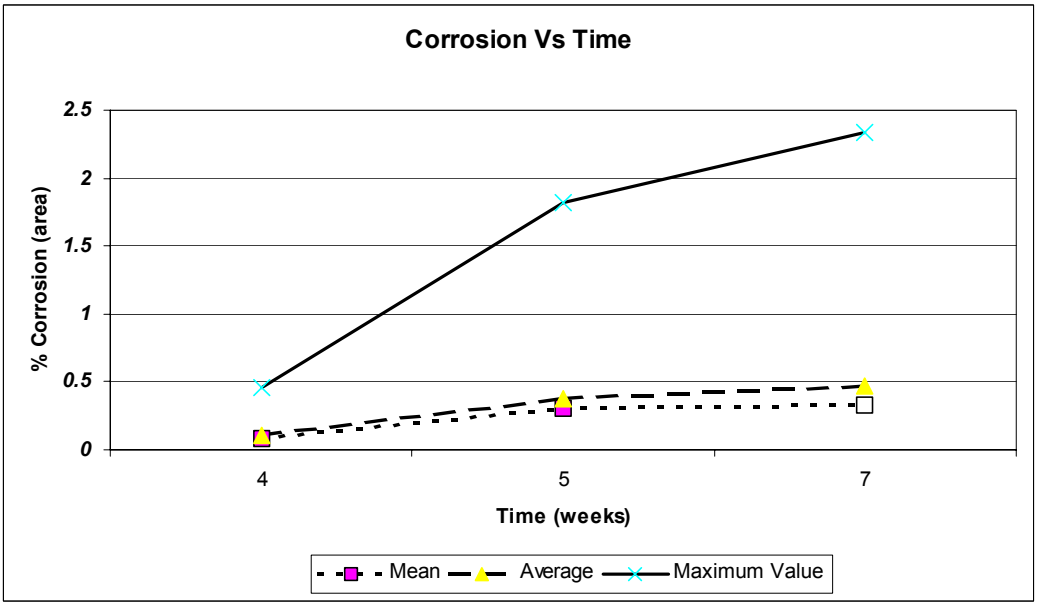

Figure 4. Percent corrosion (area loss) versus time (weeks) in a salt fog environment for 7075 T6 aluminum sheet.

Several samples were manufactured to replicate fine fatigue cracks and center thickness exfoliation corrosion. Fatigue cracks were grown from small stress intensifiers such as tool cuts in the aluminum sheet; the cracks were grown by utilizing fatigue machines to elastically stress the samples. Several methods for producing exfoliation corrosion samples were attempted. Unsuccessful methods included joining two thin plates together with one of the plates having surface discontinuities (flat bottom holes) on it. Methods for joining the two plates included grease, glue, and metal filled epoxy cement. One method that appeared to be highly successful was drilling a flat bottom hole in a sample and then welding over the hole making sure that the depth of the weld pool didn't reach the bottom of the drilled hole. This resulted in a solid sample with a centerline discontinuity, simulating exfoliation corrosion.

Samples were also manufactured to simulate single corrosion pits under paint. Flat bottom holes with dimensions 0.03 inches in diameter and depths varying from 0.010 inches to 0.05 inches were placed in an array. The samples were then coated with standard paint in such a way that one set of holes having the full range of depths was covered by one paint thickness (2 mils), two paint thicknesses (4 mils), and three paint thicknesses (6 mils).

Real-Time Ultrasound Imaging

In order to perform real-time ultrasound imaging, a concept was developed by Imperium Inc. wherein sound waves could be imaged in a water media using a modified infrared charge coupled device (CCD). Since then, continued development of the "Acoustocam" system has taken place in partnership with Naval Aviation (NAVAIR) through small business innovative research (SBIR) contracts and the current SERDP project.

The basis of the real-time ultrasound imaging technology is a newly developed and patented two-dimensional piezo microelectronic array that generates high resolution subsurface c-scan images over an area in real-time. This is in contrast to present c-scan systems based on a point-by-point scans, which are time consuming and require an immersion system. Entire areas can be imaged with the new portable system in the same amount of time it would be necessary to acquire data from a single point with a standard c-scan system. Investigation and development during the two year period of the SERDP program resulted in three major inspection methods for real-time ultrasound imaging: through transmission, reflection, and angle beam.

Thermal Imaging

Thermal imaging is a nondestructive evaluation technique that relies upon heat transfer characteristics of a given material to discriminate between various regions in a sample. That is, when a material is heated by external sources (for

example, flash lamps or ultrasonic frictional heating), anomalies within the material will exhibit temperature differentials that can be detected by an infrared camera.

Active thermography

Active thermography was the approach taken by Thermal Wave Imaging to look for hidden corrosion and fatigue cracks under paint. The principle behind active thermographic techniques is to use external sources to generate heat in a sample and image the sample with an infrared camera both prior to and following the application of the external source in order to record changes in surface temperature. Three main tasks were outlined as to the approach to take in order to fully evaluate and implement active thermography for the inspection of hidden corrosion and fatigue cracks under paint. The first task involved developing an understanding of the interaction between the thermal field transients and the corrosion pits by expanding on thermal models developed at Naval Air Warfare Center Aircraft Division (NAWC-AD) for the related problem of detection of hidden corrosion under lap-joints. The second task focused on optimizing a hand held thermographic imaging system for detection of corrosion and cracks under coatings. The final task was to experimentally verify the capabilities of the new thermographic system for the detection of corrosion and cracks under paints and determine the sensitivity of the system.

Sonic thermography

Sonic thermography was the approach taken by Wayne State University to look for fatigue cracks under paint. Sonic thermography is performed by utilizing high amplitude sonic waves (typically generated from a 20 kHz ultrasonic horn) to induce vibrations within a sample thereby causing frictional heating at the crack interface; an infrared camera is used as the detector to look for temperature differentials. Because the high amplitude sonic waves spread throughout the entire sample and are not affected by the specimen's surface, there is no need to remove coatings prior to inspection.

Near-Field Microwave Imaging

Microwave crack detection techniques have received considerable attention in the past few years [1-15]. These techniques rely on investigating the reflection properties of metallic surfaces using open-ended microwave probes such as coaxial and waveguide aperture probes. The presence of a surface crack changes the reflection properties of the metallic surface. Detecting these changes, as well as their properties, render such a crack detected and its geometrical properties evaluated. One of the most important features associated with these microwave nondestructive testing and evaluation techniques is their ability to detect cracks under dielectric coatings such as paint, primer and

dielectric composites, in addition to detecting cracks filled with such materials. Therefore, these techniques render paint removal unnecessary.

Open-ended rectangular waveguide probes have been used in the past to detect the presence of corrosion in steel plates under layers of paint and primer, as well as under thick composite laminate coatings [16-17]. A microwave signal reflects completely off of a metal surface, regardless of the type of metal. Therefore, the distinction between the SERDP investigation and that of corrosion in steel plates lies solely in the potential difference between the dielectric properties of rust (Fe_2O_3) and aluminum oxide (Al_2O_3).

To determine the potential of microwave crack detection and hidden corrosion techniques, the use of two specific approaches were proposed by Colorado State University and Texas Research Institute Austin, Inc., namely, open-ended rectangular waveguide (higher-order mode) and open-ended coaxial probe techniques. These are both considered to be sensitive approaches for detecting tight surface cracks and hidden corrosion with their respective advantages and limitations.

SUMMARY

Real-Time Ultrasound Imaging

The real-time ultrasonic imaging system developed by Imperium, Inc. in collaboration with NAWC-AD has far exceeded all goals and demonstrated the feasibility of detection of light corrosion and fatigue cracks under paint utilizing a highly portable system. The system works through paint and is capable of detecting corrosion as light as 0.5% weight loss in flat (sheet) material. Three different portable units were developed for real-time ultrasound imaging, these include the through transmission system, the pulse-echo (beam splitter) system, and the oblique angle beam system. Two major accomplishments resulted from this work: (1) the first commercial aerospace unit for through transmission real-time ultrasound imaging is being fabricated for Boeing/Vertol Philadelphia, and (2) application has been made for the issuance of a patent based on the oblique angle beam system.

Thermal Imaging

The thermal imaging techniques pursued by Thermal Wave Imaging and Wayne State University were fairly successful in their ability to detect light corrosion and fatigue cracks under paint. The table below summarizes the capabilities of each of the thermographic techniques investigated as well as the advantages and disadvantages of each technique.

Table 2. Comparison of all thermal imaging techniques studied under the SERDP program.

Technique	Corrosion Detection	Crack Detection	Advantages	Disadvantages
Pulse Heating	Y	Some times	Wide area, non-contact, curvature tolerant	Requires absorbing surface
UT Excitation	not tried	Y	Wide area, strong contrast	Coupling effects, point of contact
Induction Heating	N	Y	Non-contact	Coupling variation, uniformity control
Laser Diode Heating	N	Y	Non-contact, curvature tolerant	Requires absorbing surface, low power

Of the three active thermography techniques that were evaluated, the pulse thermography technique shows the most promise for transitioning into the field. The pulse thermography system developed by Thermal Wave Imaging, Inc. under the SERDP program was designed to be fully portable and has proven to have sensitivity sufficient to detect corrosion hidden under paint. Furthermore, the ability to inspect large areas by building mosaics of many smaller individual thermographic images is viewed as being very beneficial to field inspection units. The main shortcoming of the pulse thermography system is the inability to consistently locate fatigue cracks owing to low thermal contrast between the crack and the base material. In contrast, the sonic thermography system developed by Wayne State University is very capable of locating fatigue cracks in samples, however, studies still need to be performed to determine the effectiveness of sonic thermography for the detection of hidden corrosion.

Near-Field Microwave Imaging

Extensive sets of measurements over a wide range of cracks were conducted by Colorado State University using coaxial and open-ended rectangular (higher order mode) waveguide probes. Both coated and uncoated fatigue cracks and slots were studied in this investigation. The results indicate that both probes have high potential for detecting cracks under coatings such as paint and primer. Each probe possesses its unique advantages and disadvantages. The coaxial probe was shown to easily be able to detect tight cracks under coatings of about 0.15 mm at relatively low microwave frequencies (X-band). The coaxial probe was also found to be less susceptible to edge effect issues. The open-ended rectangular (higher order mode) waveguide probe also showed the ability to detect similar cracks under like coatings, however, the issues of edge effects and small changes in the standoff distance seem to be more of a concern when using this probe.

The results of the investigation by Colorado State University and Texas Research Institute showed that there exists a high potential for detecting corrosion in aluminum under a layer of paint and primer using near-field

microwave NDT techniques with open-ended rectangular waveguide probes. This was shown in both the theoretical simulations and experimental investigations performed using laboratory designed measurement systems.

The dielectric properties of paint, primer and naturally produced aluminum oxide were measured over a wide range of microwave frequencies (2.6-18 GHz). These materials were found to have low permittivities and low loss factors. Also, it was found that dielectric properties of aluminum oxide, paint and primer are very similar to each other. This is important since it is easier to detect corrosion under paint when the dielectric properties have a greater difference when compared to each other, as is the case with steel corrosion.

RESULTS AND DISCUSSION

Real-Time Ultrasound Imaging

The basis of the real-time ultrasound imaging technology is a newly developed and patented two-dimensional piezo-microelectronic array that generates high-resolution subsurface c-scan images over an area in real-time. This is in contrast to present c-scan systems based on a point-by-point scan, which is time consuming.

When measuring ultrasound energy reflected from targets of interest, particular interest is placed on the surface uniformity of the reflecting target. Specular reflection occurs when the roughness of the target is less than the wavelength of the ultrasound in the medium in which the ultrasound is propagating. For example, if the energy is reflected from a smooth back surface of the target, the energy will be reflected specularly. On the other hand, if the surface is appreciably corroded, scattering will take place. An internal crack will also act as a scattering source.

Scattered energy is typically difficult to detect by a point detector since most of the energy will not strike the detector. However, if a lens is incorporated in the ultrasound camera, the ultrasound receiver will collect much of the energy. Thus, it is quite possible for the ultrasound camera system to detect energy scattered from internal faults that could not otherwise be measured.

Through transmission

Initial work in the area of real-time ultrasound inspection was performed using through transmission techniques. In the through transmission technique a sound beam (coming from an ultrasonic transducer) is passed through a sample from one side and detected by the ultrasound camera on the other side of the sample. Early equipment required the use of an immersion tank so that the transducer, test sample, and camera diaphragm could be immersed in water to permit

efficient transmission and detection of the sonic waves. A photograph of the system and immersion tank is shown in Figure 5.

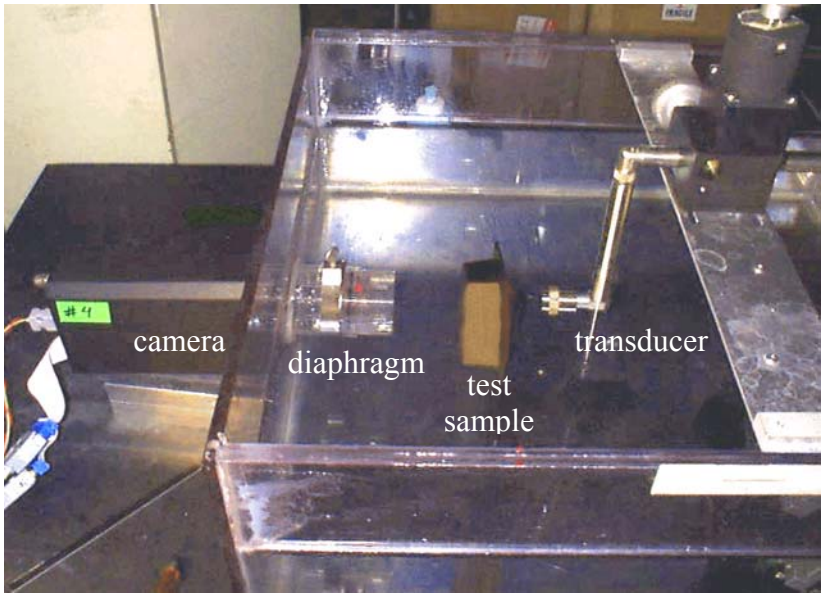

Figure 5. Immersion tank and early through transmission real-time equipment.

Set-up of the immersion tank involved mounting an aqualene diaphragm on one end of the tank as the ultrasound camera was manufactured with a block of aqualene cemented on the imaging chip. In order to obtain an image, a suitable liquid or gel was applied to the outside surface of the diaphragm and the camera was moved into contact with the diaphragm. An immersible transducer (Panametrics A409S-SB 5 MHz usually) was aimed directly into the camera chip and the test sample (target) was positioned near the transducer. The lens array of the camera was then adjusted to focus slightly in front of the transducer. Early through transmission results showed excellent clarity and the ability to penetrate composites up to an inch thick, showing details as fine as the fibers themselves. See Figure 6.

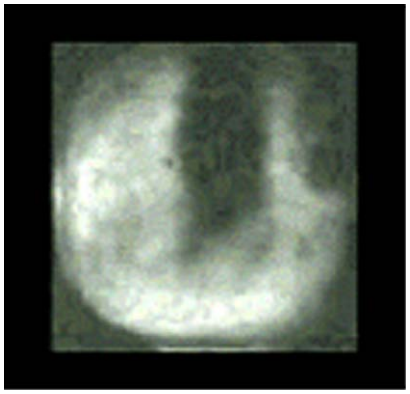

Figure 6. Through transmission real-time ultrasound image of a composite panel with included flaws showing the detail available at high inspection speed.

Improvements gained through study of the physical principles of ultrasound and application to the imaging of ultrasonic waves led to continuous improvements in the techniques used. Higher resolution and clarity were achieved by making modifications to various components in the imaging system, including modifications to the 100 series Acoustocam camera chip, physical coupling, lenses, and transducers. By way of example, the resolution of a millimeter scale focused in through transmission is shown in Figure 7. This resolution and clarity far exceeds anything achieved to date by other ultrasonic methods and the speed of inspection is without comparison.

Figure 7. Through transmission real-time ultrasound image of a plastic millimeter scale.

The detection of very light corrosion in the through transmission mode was easy to accomplish through many layers of paint on either the front or back surface. (See Figure 8.) The one drawback of this system was the requirement that the test component, camera diaphragm and transducer all needed to be immersed in water. Few components in the aerospace industry lend themselves to total immersion and as such Imperium Inc. worked on the fabrication of a fixture for the inspection of parts by through transmission without a water tank. The fixture consists of a large C-shaped frame with the transducer on one side and the camera of the other (Figure 9). Although the use of a couplant (thin film of water or gel) is still necessary in order for the sound energy to pass through the sample from the transducer to the camera diaphragm, the new system is far more amenable to the inspection of aerospace components and other parts where total water submersion may not be possible.

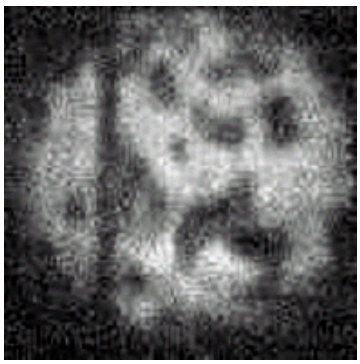

Figure 8. Detection of light corrosion in aluminum 7075 T6 panel.

Figure 9. Acoustocam through transmission real-time ultrasound imaging system in C-shaped frame.

The through transmission method for real-time ultrasound imaging has gained the quickest success and approval by the aerospace industry. In fact, Boeing Vertol is currently evaluating Imperium's Acoustocam through transmission system for use in inspecting small composite parts for delaminations and defects in the production environment.

Reflection

The reflection method of real-time ultrasonic inspection developed during the SERDP program has progressed from a concept to a reality. The inspection camera developed is portable and has a diaphragm on the end that can be pushed against a slightly wetted surface to image the interior of a part. A schematic drawing and a photograph of the beam splitter reflection camera are shown in Figure 10 and Figure 11 respectively, and its operation is described below. In the reflection method the sound generated from an unfocused transducer is redirected into the test sample at the 50/50 beam splitter. The sound propagates into the test sample and upon encountering a discontinuity (e.g. corrosion or crack) or the back wall of the test sample is reflected back into the camera. The sound beam then travels through the beam splitter and focusing lenses to the camera chip. Inspection of corrosion samples prepared in the laboratory show that corrosion pits one to three mm in diameter are capable of being detected without paint removal from either the front surface (Figure 12) or the back surface of the test sample in real-time.

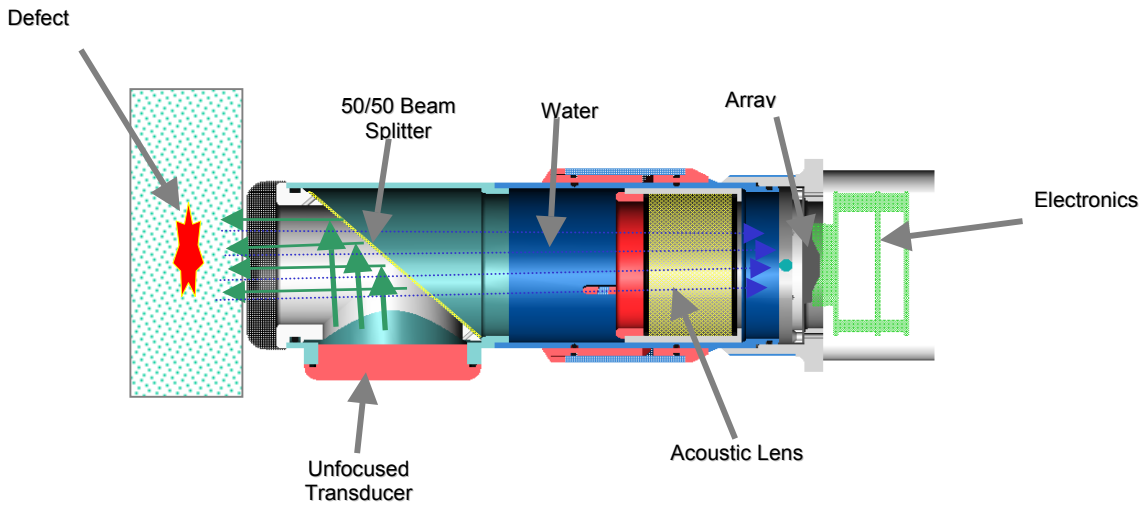

Figure 10. Schematic drawing of beam splitter reflection camera.

Figure 11. Photograph of Acoustocam beam splitter camera.

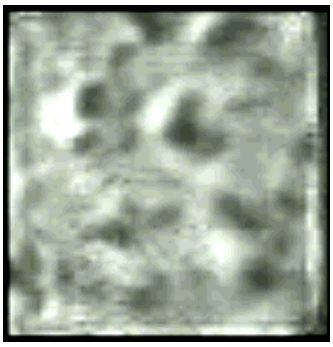

Figure 12. Corrosion pits (1 mm diameter) detected using Acoustocam beam splitter camera viewed from the front surface of the sample through paint.

During the course of the SERDP program many changes were made to advance the technology for real-time reflection ultrasound imaging. The electronics necessary to operate the beam splitter Acoustocam reflection camera shrank from a large rack mount panel to a package the size of a pack of playing cards mounted on the end of the unit. Changes in lens design helped to achieve higher resolution and changes in the beam splitter panel increased the clarity and strength of the received signal. A schematic of the re-designed beam splitter Acoustocam reflection camera is shown in Figure 13.

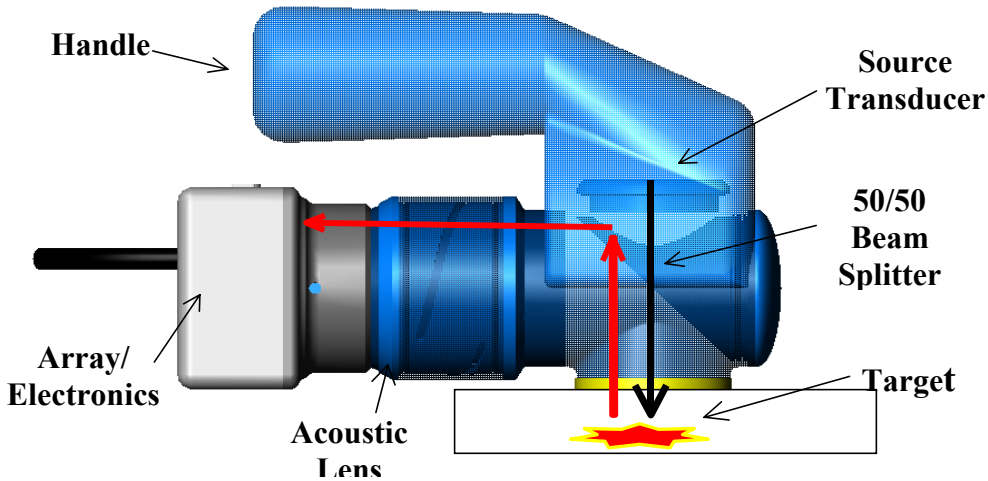

Figure 13. Schematic of re-designed beam splitter reflection camera.

The reflection method is best suited for the inspection of components where only one side of the component is available to the inspector. The real-time reflection ultrasound camera has been found to be of great utility in the inspection of composite components as well as metallic ones. One such application is the inspection of honeycomb panels for locating areas of delamination caused by fabrication problems, fatigue, or water intrusion (Figure 14). Inspection of such components is quite difficult for techniques based on point inspection methods such as the focused beam c-scan ultrasonic method that uses a small ultrasonic beam and scans very slowly over a structure to allow a computer to build up a picture of the interior. The Acoustocam reflection method is analogous to a visual inspection in which one looks into the interior with a field of view greater than one inch in diameter. The speed of the inspection is very rapid compared to all other existing ultrasonic inspection methods.

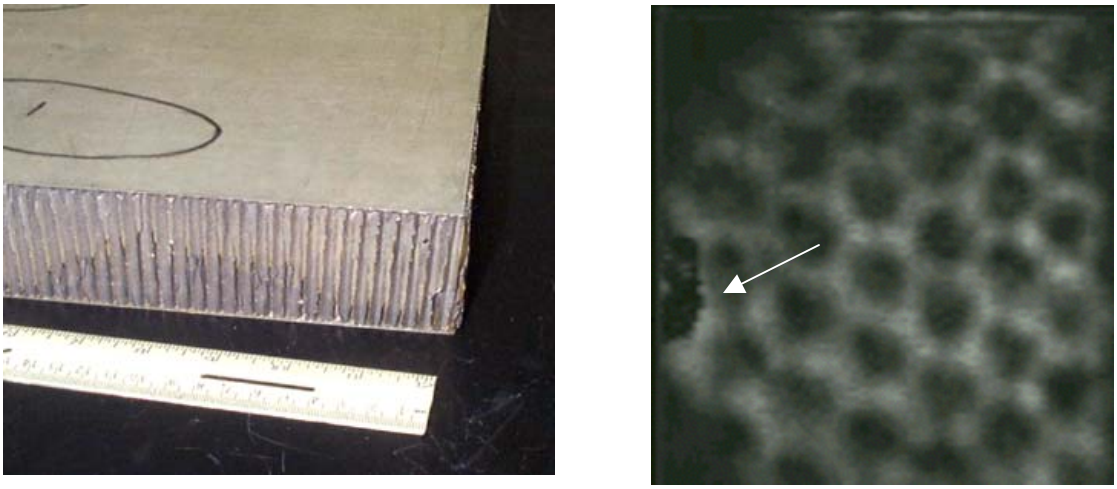

Figure 14. Honeycomb sample (left) and debonding (right) that has occurred within the sample as detected using the reflection Acoustocam system.

Angle beam

The inspection of very thin metallic sheets (0.06 inches up to 0.125 inches thick) was shown to be difficult for the reflection method of ultrasound imaging to undertake; this was due to the extremely short time delay between the front and back surfaces of the thin sheets. By injecting the sound beam into the metallic sheet at an appreciable angle it was found to cause multiple reflections progressing along the sheet with the end result of illuminating a large region of the sample with sound energy (Figure 15). A prototype angle beam ultrasound camera was fabricated at the Becker Labs of the Naval Air Warfare Center Aircraft Division (Figures 16-17) and has proven that rapid ultrasound imaging of thin sheet is practicable and is unaffected by painted coatings (Figure 18).

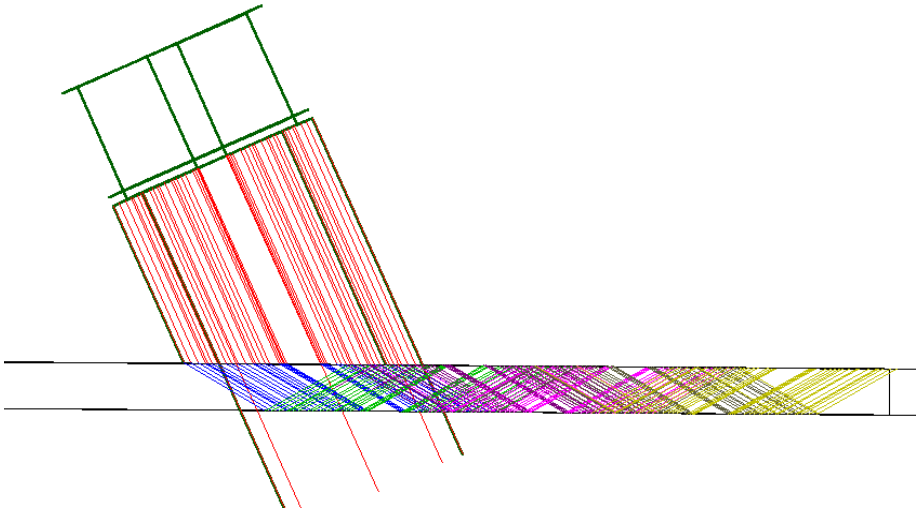

Figure 15. Modeling was used to examine the beam inside a plate during one side inspection using the oblique angle reflection method.

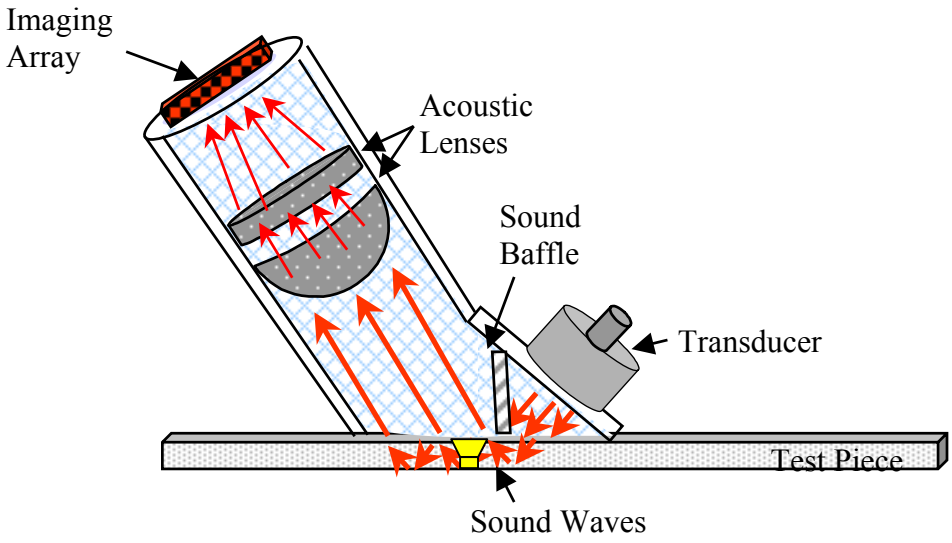

Figure 16. Schematic of oblique angle reflection camera for real-time ultrasound imaging.

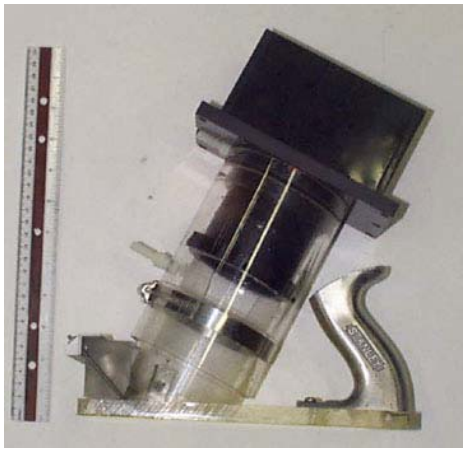

Figure 17. Photograph of prototype oblique angle reflection camera.

Figure 18. Corrosion hidden under paint as imaged with the angle beam reflection camera.

The Acoustocam system was shown to be able to respond to the dynamic range of the multiple bounces with an image very similar to that of a through transmission image with the exception that recurring images of a defect are observed in the oblique angle reflection mode owing to the fact that the sound beam continues to reflect. (See Figure 19). The concept, however, has proven to be viable for the inspection of corrosion under painted coatings at high speed and with high sensitivity. Application has been made for the issuance of a patent based on the oblique angle beam system.

Figure 19. Angle beam image of a flat bottom hole showing the multiple images that occur.

Thermal Imaging

Thermal imaging is a nondestructive evaluation technique that relies upon heat transfer characteristics of a given material to discriminate between various regions in a sample. That is, when a material is heated by external sources (for example, flash lamps or ultrasonic frictional heating), anomalies within the material will exhibit temperature differentials that can be detected by an infrared camera.

Three main tasks were outlined as to the approach to take in order to fully evaluate and implement thermal imaging for the inspection of hidden corrosion and fatigue cracks under paint. The first task involved developing an understanding of the interaction between the thermal field transients and the corrosion pits by expanding on thermal models developed at Naval Air Warfare Center Aircraft Division (NAWC-AD) for the related problem of detection of hidden corrosion under lap-joints. The second task focused on optimizing a hand held thermographic imaging system for detection of corrosion and cracks under coatings (Thermal Wave Imaging). The final task was to experimentally verify the capabilities of the thermographic systems for the detection of corrosion and cracks under paint and determine the sensitivity of the systems (Thermal Wave Imaging and Wayne State University).

Modeling thermal field transient interaction with corrosion pits

The effects that materials and process parameters have on thermal contrast have been previously determined. These parameters include the amount of heat (Q) deposited on the surface the sample, of the pit size (A) and depth (h), of the substrate thickness (t_o), of the lateral thermal conductivity (k_l), of the coating thermal properties and of the heating rate (Q/τ). This combined effect can be summarized in the following formula and the following statements:

$$\Delta T = \frac{Q}{\rho c}\left(\frac{1}{d} - \frac{1}{t_o}\right)\left[\frac{k_n R^2}{4k_L}\left(\frac{t_o}{d(t_o - d)}\right)^2\right]^{\frac{1}{1-\frac{k_n R^2}{4k_L}\left(\frac{t_0}{d(t_0-d)}\right)^2}}$$

- The contrast temperatures (T) increase linearly with the amount of energy deposited per unit area (Q).
- The higher the specific heat-density of a material ($c\uparrow$) the smaller the contrast temperatures becomes ($T\downarrow$)
- The closer the defect is to the surface ($d \to 0$) the larger that the front contrast temperature becomes ($T_{front} \to \infty$) while the back contrast temperature is independent of d.
- As the defect depth approaches the panel thickness ($d \to t_o$) the front contrast temperature vanishes ($T_{front} \to 0$) while the back contrast temperature is constant.
- For a given defect depth d, the thicker the panel ($t_o \to \infty$) the larger the front contrast
- As defects approach to the surface ($d \to 0$) or as they approach the far end ($d \to t_o$), the lateral heat effects tend to disappear ($f_{lateral}$ (d) $\to 1$) and the contrast is given by $\Delta T = \frac{Q}{\rho c}\left(\frac{1}{d} - \frac{1}{t_o}\right)$
- When the defect size decreases ($R \to 0$) or the lateral conductivity increases ($k_L \to \infty$), then the lateral heat factor vanishes ($f_{lateral}$ (d) $\to 0$) and the thermal contrast disappears ($T \to 0$)
- When the lateral conductivity decreases ($k_L \to 0$) or the defect size increases ($R \to \infty$) then we approach lateral isolation ($f_{lateral}$ (d) $\to 1$) and the contrast becomes $\Delta T = \frac{Q}{\rho c}\left(\frac{1}{d} - \frac{1}{t_o}\right)$
- When the thickness of the panel becomes very large ($t_o \to \infty$) then the contrast temperature has the limiting value given by $\Delta T = \frac{Q}{\rho c}\frac{1}{d}\left(\frac{R^2}{4d^2}\right)^{\frac{1}{1-\frac{R^2}{4d^2}}}$

- The higher the specific heat-density product of the second layer ($c_2\uparrow$) and/or the smaller the specific heat-density product of the first layer ($c_1\downarrow$) the larger the contrast temperature becomes ($T_{front}\uparrow$)
- The optimum heating time is given by $\tau_1 = \frac{\rho c}{k}\left(\frac{d(t_o - d)}{t_o}\right)^2$
- If the heating time exceeds the quantity given by $\tau_2 = \frac{\rho c}{k_L}\frac{R^2}{2}$, then the thermal contrast will be exponentially diminished.

All the parameters provided in the previous statements and in the equations are represented in Figure 20. One of the key results of all this modeling is the capability to generate a detectability map. This type of map shows the region in the parameter space (defect depth vs. defect diameter) where defects (corrosion pits) can be detected and regions where they cannot be detected for a given experimental condition. Figure 21 shows a typical example of a detectability curve for two different aluminum panels. The x-axis represents the flaw diameter (2R). The y-axis represents the defect depth (d). The broken straight lines represent two panel thicknesses. The broken straight line with the label t=1/16" represents an aluminum panel thickness of 1/16" = 0.0625". A point below that line will characterize a defect of specific length and depth in that panel. The broken curve shown on that same graph and located just under the straight line separates that surface area into two regions. One region is labeled detectable region while the remainder region is labeled the undetectable region. The detectable region represents the defects that can be detected thermographically with the infrared system at NAWC-AD. The undetectable region represents the defects that cannot be detected thermographically with the system at NAWC-AD.

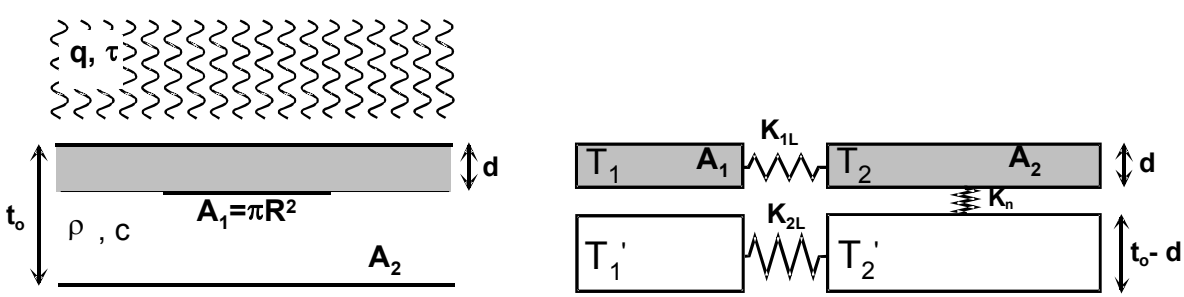

Figure 20. This figure shows the building blocks of the simple calorimetric model. Two different materials with different density and specific heat comprise the panel.

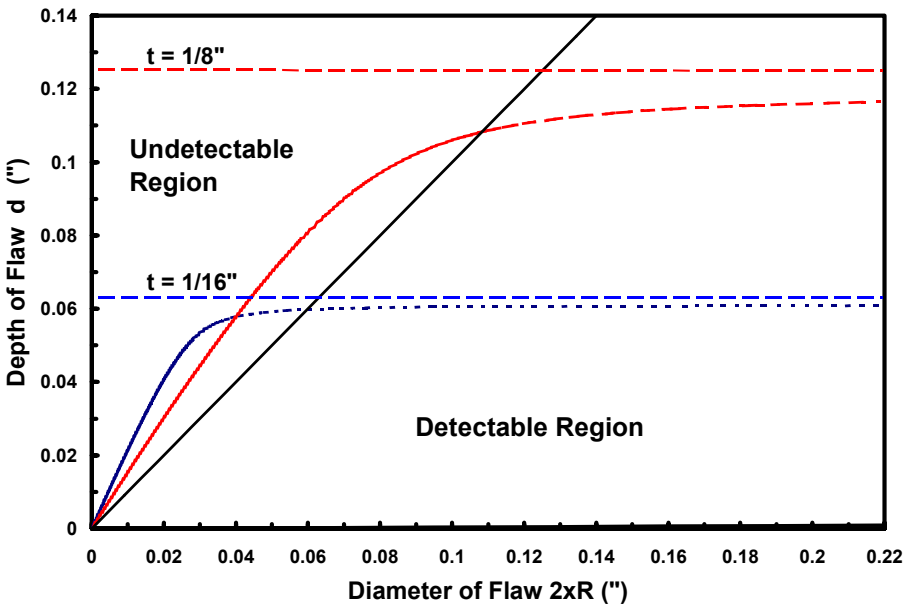

Figure 21. Graph showing the thermal imaging detectability regions in parameter space for two different aluminum panel thicknesses.

From Figure 21, it becomes clear that not all of the pits will be thermographically detectable. The following remarks can be made by analyzing Figure 21:

- No matter how large the defect might be, there is a defect depth (or defect shallowness) below which defects cannot be detected. For 1/16" thick aluminum panels that depth corresponds to approximately 5% mass loss. For a 1/8" thick aluminum panels that corresponds approximately 10% mass loss. The only way by which shallower defects might be detected would be by increasing the amount of energy deposited on the surface.

- As the defect cross section decreases, a point is reached where the detectability limit changes from being flat and constant to rapidly decreasing towards zero. In the case of a 1/16" thick aluminum panel that transition point corresponds to approximately 2R = 40 mil. For a panel that is 1/8" thick the transition point where the detectability starts departing from a constant value is approximately 100-mil diameter.

- As the panel thickness increases the ratio of "detectable" to "non–detectable" regions decreases as well as the transition point from constant detectability limit to rapidly decreasing detectability increases becomes larger. Both of these limitations reduce the effectiveness of corrosion detection for thick materials.

- In order to improve the detectability region curve for a material, larger amounts of energy need to be deposited on the surface of the panels.

Figure 22 below shows two panels with flat bottom holes (FBH) used to characterize the response of the thermographic system. The panel on the left is a 1/8” thick panel while the panel on the right is a 1/16” thick panel. The panel on the left has a total of 40 FBH while that on the right has a matrix of 12 FBH. The largest flat bottom hole on the left panel was 1” in diameter while the smallest hole diameter was 1/8” diameter. The brightest regions correspond to 80% mass removal while the dimmest regions correspond to 10% mass removal. The largest flat bottom hole on the right panel was 1/16” in diameter while the smallest diameter was 1/32” diameter. The brightest regions correspond to 80% mass removal while the dimmest regions correspond to 40% mass removal. It is clear from the panel on the right that the smaller the diameter of your FBH the smaller the contrast, in fact, the 3/64” diameter and the 1/32” diameter can not be seen in the image at any of the depths studied.

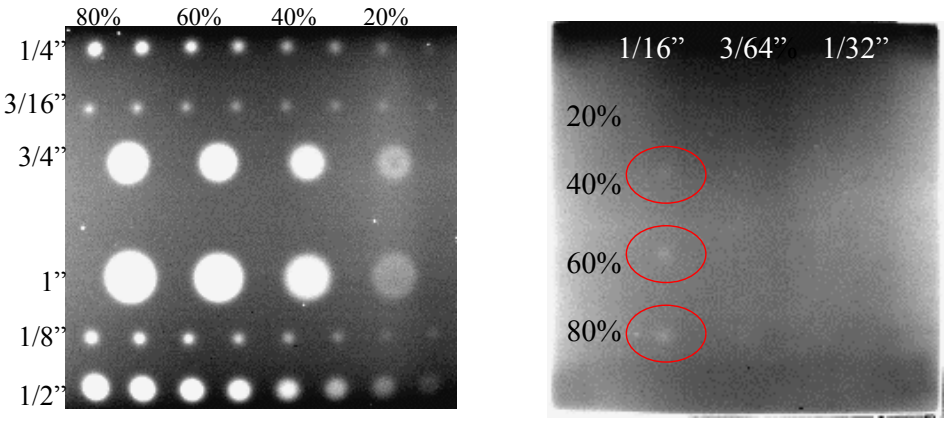

Figure 22. Aluminum panels with flat bottom holes used to characterize the response of the thermographic system. The panel on the left is 1/8” thick and has 40 flat bottom holes of different radii and depths. The panel on the right is 1/16 “ thick and has 12 flat bottom holes with much smaller diameters.

Optimization of the thermographic imaging system

Thermal Wave Imaging completed the development of an advanced portable thermographic imaging system with Navy SBIR Phase II funding. A photo of the complete system is shown in Figure 23. The system has many advantages compared with previous generations including, improved lateral resolution, controls that are accessible from the camera head, an LCD display panel located on the camera head, lighter weight, and the system allows for single operator use. In addition, Thermal Wave Imaging developed sophisticated software with automatic detection, segmentation, and classification algorithms for corrosion inspection. Improvements were also made in the data processing, functionality, and storage capabilities of the thermographic system. The advanced portable thermographic imaging system was used in the SERDP program to evaluate the use of thermal imaging for the detection of hidden corrosion and fatigue cracks.

Figure 23. Thermographic inspection system developed by Thermal Wave Imaging, Inc.

Thermal Wave Imaging has investigated several methodologies for conducting active thermography studies for the detection of corrosion and fatigue cracks hidden under paint, these methodologies include, asymmetric inductive heating, asymmetric laser diode heating, sonic excitation heating, and thermal pulse excitation heating. The first two methods rely upon depositing energy near the crack in an asymmetric pattern so as to initiate lateral heat flow. Under these conditions it is expected that a crack will offer the maximum thermal resistance and therefore the largest likelihood that a thermal contrast will develop across the crack.

Figure 24 shows a fatigue crack that was generated in the laboratory for the purpose of comparing all the thermographic excitation techniques. A 1/16" x 3" x 12" aluminum panel was cut with a Dremel® tool to introduce a small notch in the center of the panel. The sample was placed under bending loads in a fatigue machine until fatigue cracks developed. Figure 24 shows the Dremel® notch and two cracks emanating from the tips of the mark. The fatigue cracks are barely visible to the eye and require special illumination to make them visible. The total length of the crack is approximately ½" and it is not a through crack.

Active thermography

Active thermography was the approach taken by Thermal Wave Imaging, Inc. to look for hidden corrosion and fatigue cracks under paint. The principle behind active thermographic techniques is to use external sources to generate heat in a sample and image the sample with an infrared camera both prior to and following the application of the external source in order to record changes in surface temperature. Three methods for performing active thermography were evaluated by Thermal Wave Imaging, Inc., inductive heating, laser diode heating, and pulse

thermography. These methods are described in detail below along with the capabilities/shortcomings of each technique.

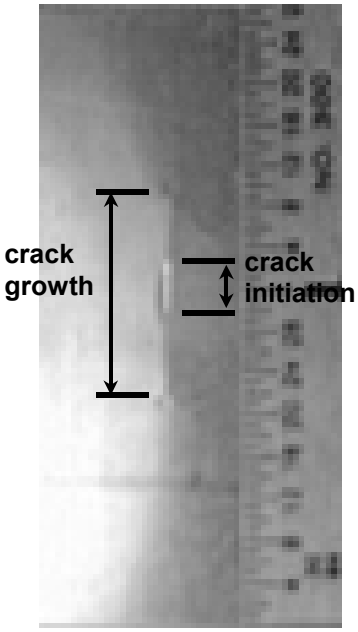

Figure 24. Aluminum panel with a fatigue crack in the center.

Inductive heating

Figure 25 shows the experimental setup used for the inductive heating method of thermographic imaging. The key component is the induction head and the induction coil at the center of the photograph (the power supply is not shown). The induction coil consisted of two loops of thin wall copper tube through which water flowed for cooling purposes. A typical thermographic image of the fatigue crack specimen as acquired using inductive heating is shown in Figure 26.

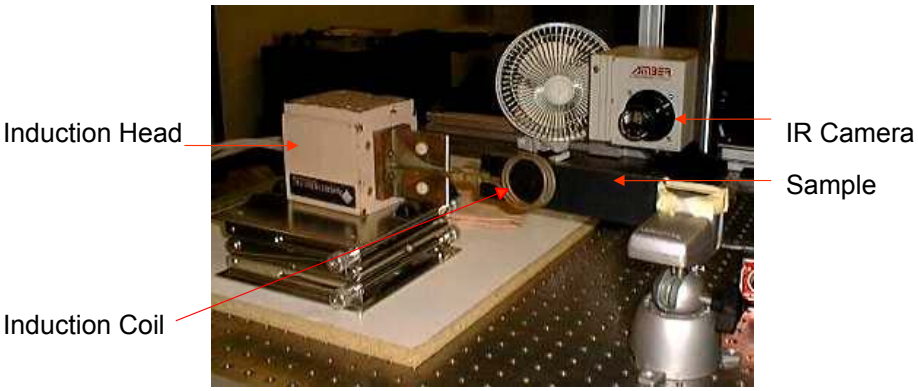

Figure 25. Experimental setup for the inductive heating excitation method of thermal imaging.

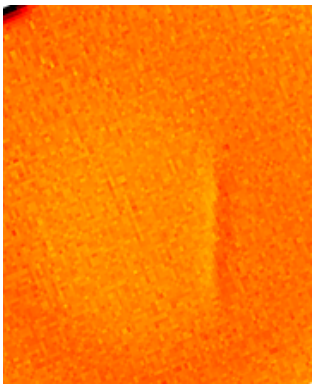

Figure 26. Thermal contrast generated across the fatigue crack by inductive heating.

Several problems were identified with the induction method of thermal excitation. First, the power requirements were significant making the equipment too heavy to be considered portable. The high power requirements mandated that the induction coil be cooled, adding weight and other complications (rigid coil, water tubing) to the system. The rigidity of the coil did not allow for small coils, and therefore small localized heating effects. As a result the thermal gradients were not large in general, leading to small thermal contrast. Finally, with the high power requirements, electrical shock protection became an issue. In general it was determined that the induction thermal excitation method would require significant developmental work in order to increase sensitivity and as such other thermal excitation methods were investigated.

Laser diode excitation

Figure 27 shows the experimental setup used for the asymmetric laser diode heating method; the key component of the system is the relatively economic laser diode shown in the photograph. The laser is located behind the camera lens. It should be noted that the power supply for the laser is not shown in Figure 27. Figure 28 represents the thermal contrast image obtained from the fatigue specimen following data massaging. This technology has several advantages and some disadvantages compared to the inductive heating method. One advantage of the laser diode heating method is that the laser diode and power supply are small which allow the system to be portable. Due to the natural collimation of laser beams, the heated area can be relatively small, and the thermal gradients can be high enough to produce thermal contrast. The major problem with this type of system is the power of the laser diode, which tends to be small leading to small thermal contrast over large areas.

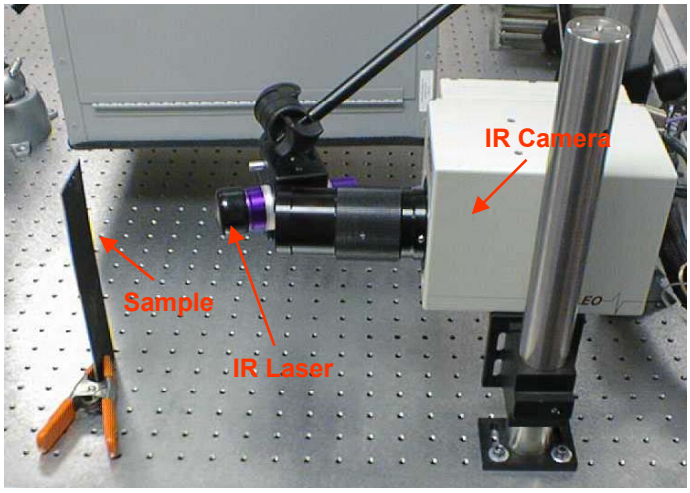

Figure 27. Experimental setup for laser diode heating excitation method of thermal imaging.

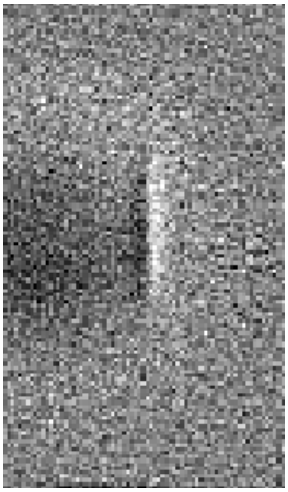

Figure 28. Thermal contrast generated across the fatigue crack by laser diode excitation.

Pulse thermography

A schematic diagram of the pulse thermography approach is shown in Figure 29. The basic concept of this heating method is to use a strong thermal pulse in conjunction with infrared imaging proceeding and following the pulse to record differences in surface temperatures.

Several issues needed to be resolved before the pulse thermography system could be used to look for the effects of corrosion hidden under paint. Detector saturation due to flash heating initially masked the corrosion under the paint, therefore the flash energy was reduced and the dynamic range of the camera

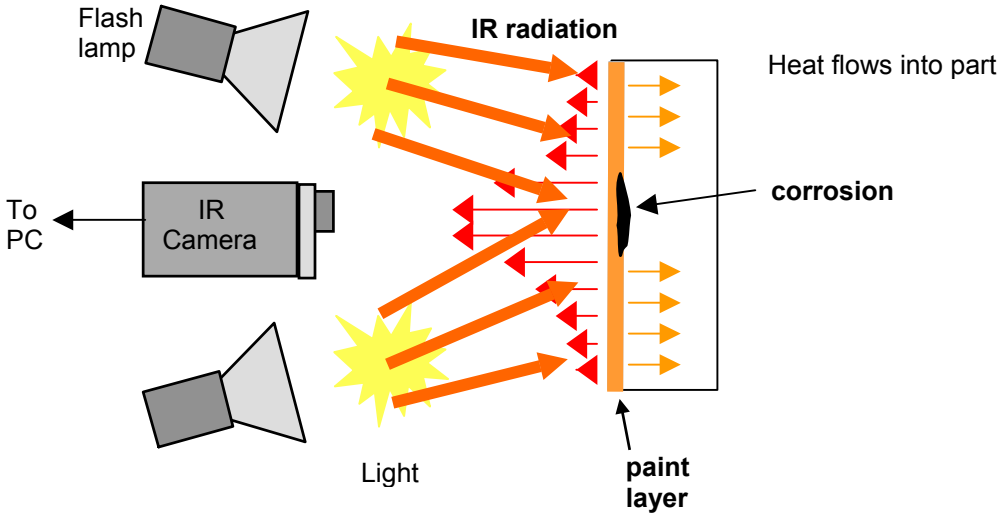

Figure 29. Schematic diagram of the experimental setup for pulse thermography.

was matched to the early time domain only (later time domains require higher flash energy). In addition, changes needed to be made in order to distinguish corrosion from flash reflection artifacts. These changes involved using thermal decay characteristics to identify reflection and corrosion signatures. As a result of these modifications it was possible to identify regions of hidden corrosion under painted surfaces; see Figure 30. Furthermore, as can be seen in Figure 31, it was possible to image large specimens by building a large composite image from smaller individual pulse thermographic images.

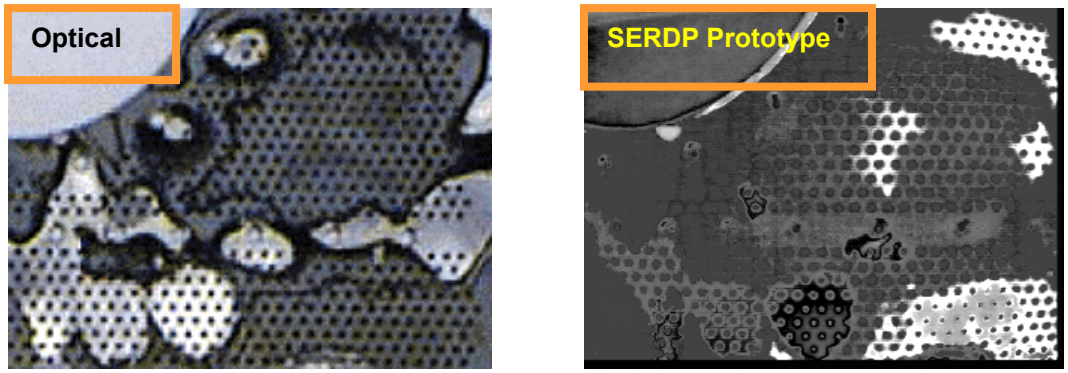

Figure 30. The image on the left shows an optical photograph of an F-18 intake panel in which areas of previously detected corrosion have been ground out. The panel was discolored and had numerous stains. The white areas observed in the thermographic image on the right show regions where corrosion was detected under paint using an optimized pulse thermography system (3 kJ flash energy, 6 oz. uncooled camera, optimized signal processing).

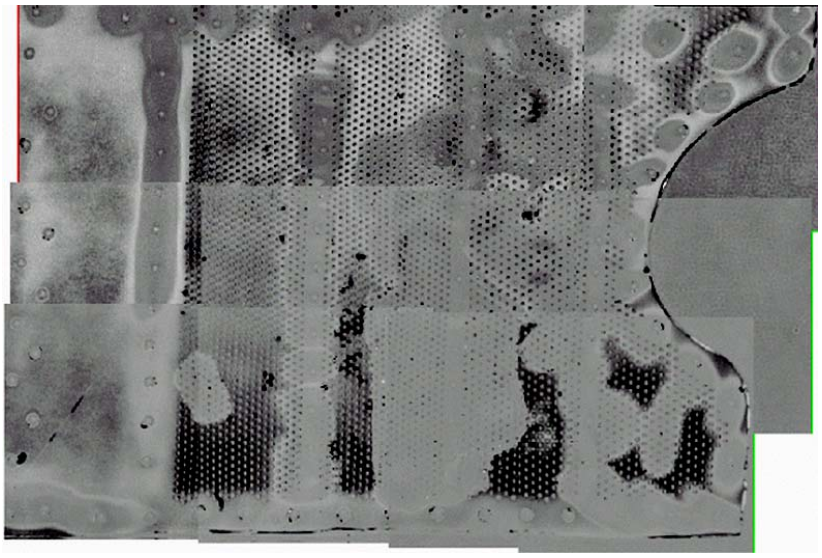

Figure 31. Large composite thermographic image of F-18 intake panel created from 8 smaller individual images.

Sonic excitation

Sonic thermography was the approach taken by Wayne State University to look for hidden corrosion and fatigue cracks under paint. Sonic thermography is performed by utilizing high amplitude sonic waves (typically generated from a 20 kHz ultrasonic horn) to induce vibrations within a sample thereby causing frictional heating at an interface (e.g. a crack); an infrared camera is used as the detector to look for temperature differentials. Because the high amplitude sonic waves spread throughout the entire sample and are not affected by the specimen's surface, there is no need to remove coatings prior to inspection. In addition large areas with complex curvature can be imaged with the system in the same amount of time that it takes to acquire a single point with a standard c-scan system.

Figure 32 shows the experimental setup used for the sonic excitation method. The main component of this system is the ultrasonic horn used to impart the sonic energy. Figure 33 shows a thermal image acquired from the fatigue crack specimen after only 2 seconds of excitation with the ultrasonic horn. Clearly thermal contrast is very good.

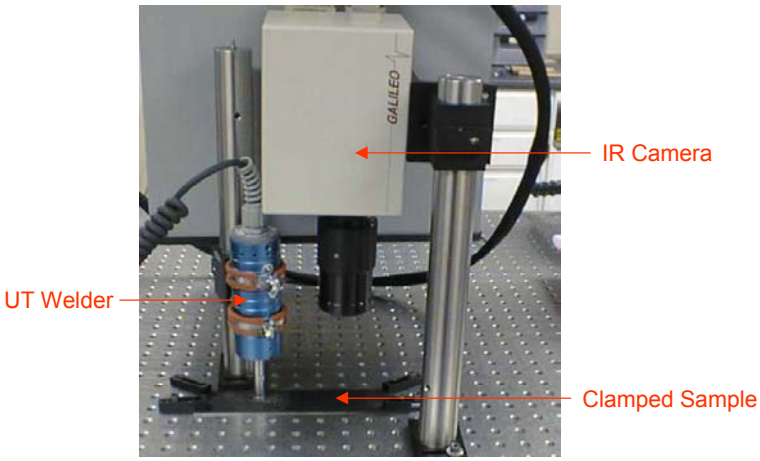

Figure 32. Experimental setup for the sonic excitation method of thermal imaging.

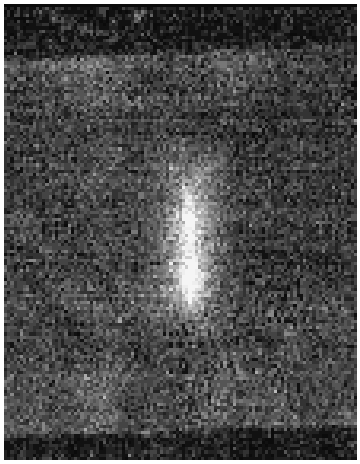

Figure 33. Thermal contrast generated on the fatigue crack specimen by sonic excitation.

Near-Field Microwave Imaging

The presence of surface discontinuities such as cracks or corroded regions change the reflection properties of a metallic surface, by using microwaves to detect these changes and the associated materials properties the discontinuity is distinguished and its geometrical properties evaluated. One of the most important features associated with microwave nondestructive testing and evaluation techniques is the ability to detect cracks and corrosion under dielectric coatings such as paint, primer and dielectric composites, in addition to detecting cracks filled with such materials. Therefore, nondestructive microwave inspection techniques render paint removal unnecessary.

To determine the potential of microwave crack detection and hidden corrosion techniques, the use of two specific approaches were proposed by Colorado State University, namely, open-ended coaxial probe and open-ended rectangular waveguide (higher-order mode) techniques. Both of these techniques are considered to be sensitive approaches for detecting tight surface cracks and hidden corrosion with their respective advantages and limitations.

Open-ended coaxial probe

Figure 34(a) and 34(b) show the side and plan views of an open-ended coaxial microwave probe [13]. In general, when open-ended aperture probes interact with material media the aperture fields are perturbed as a function of the properties of the medium they are interacting with. Consequently, a certain amount of the incident fields will be reflected back into the probe. The properties of this reflected signal, directly or its comparison with the incident signal (reflection coefficient) or its combination with the incident signal (standing wave), can provide information about the presence of the material and any anomalies in it as well as giving information about the properties of the anomaly (such as crack dimensions). The distribution of the electromagnetic fields at the aperture of a given open-ended probe significantly influences its interaction with a given anomaly.

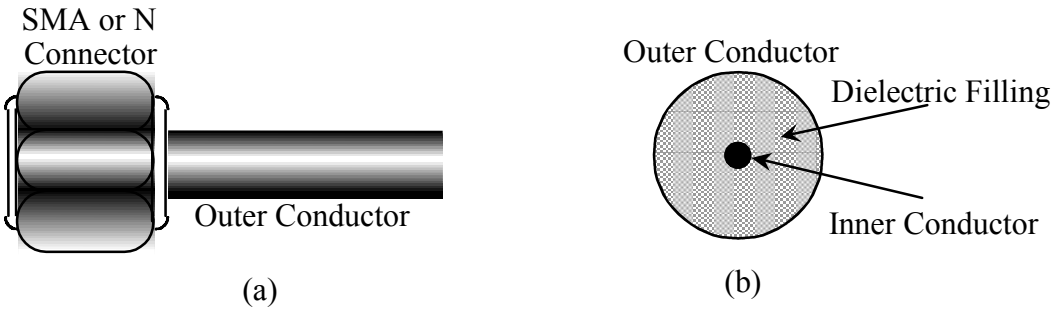

Figure 34. (a) Side view and (b) plan view of an open-ended coaxial microwave probe.

When the coax is terminated in a metal plate (conducting plate) the entire incident signal gets reflected back into the coax. As the crack appears in the aperture, the electric field distribution (and hence induced surface currents) is perturbed, which subsequently change the properties of the reflected signal. As more of the crack enters the aperture more of this perturbation is experienced. As the crack passes over the inner conductor the opposite is experienced [13]. The change in reflected signal can be detected in several fashions. One may measure the reflection coefficient at the coaxial aperture and use the change in its phase or magnitude as a means for detecting a surface crack. It is also possible to use systems sensitive to phase or amplitude of reflection coefficient that produce a dc voltage proportional to the change in the phase of magnitude

of reflection coefficient. For the experiments conducted in the SERDP program the latter method of detection of change in reflection signal was utilized.

Open-ended rectangular probe

Figure 35 shows a side view of the open-ended rectangular waveguide probe. In the same manner as described with the open-ended coaxial probe, when an open-ended rectangular waveguide is terminated by a metal plate the incident signal goes through a complete reflection. The incident signal is that of the dominant TE10 mode in a rectangular waveguide [3, 10]. However, when there is a crack in the metal plate the surface currents on the metal plate are disturbed and high-order modes are generated. The presence of these modes changes the properties of the reflected signal, hence changes the reflection coefficient (in particular its phase) [3, 10]. The change in phase can be detected somewhere in the waveguide away from the metal plate. This type of crack detection is known as the dominant mode approach. However, it is also possible to detect the presence of the evanescent higher-order modes by placing a small probing antenna near the waveguide aperture. These modes possess all three electric field components. Thus, when the antenna probe is directed along the x-axis it picks up electric field components in that direction. In the absence of a crack there are no high-order modes generated. However, in the presence of a crack higher-order modes are generated and picked up by the small antenna placed along the narrow dimension of the aperture. This signal is then detected using a diode detector.

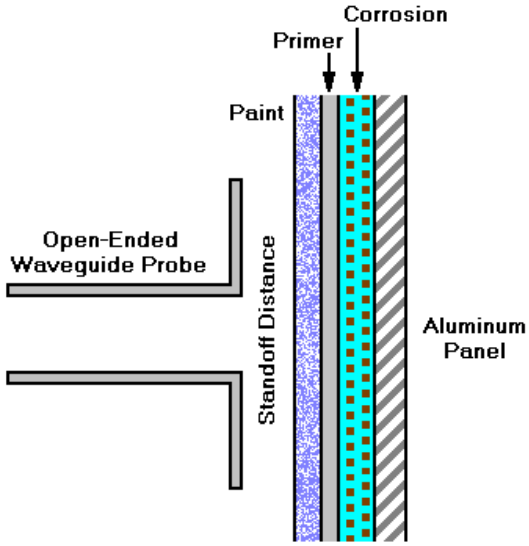

Figure 35. Schematic of open-ended rectangular waveguide used for detecting fatigue cracks and corrosion under paint.

Detection of fatigue cracks

Due to the fact that samples were not supplied by the sponsor of this research samples were manufactured by investigators at Colorado State University. Cracks of varying sizes were generated in aluminum plates using jeweler saws (more like slots). Some of the samples were fatigued in order to grow the cracks to better mimic fatigue cracks of concern in the field. In order to simulate paint of varying thicknesses, specimens were covered with tissue paper, tape and paint.

During the scanning process using the open-ended coaxial probe, the phase change in the reflection coefficient with respect to when the crack is out of the coax aperture, or the voltage proportional to this was recorded. This voltage as a function of the scanning distance is called the *crack characteristic signal*. Figure 36 (a) and 36 (b) show the influence of crack size and coaxial aperture dimension on the crack characteristic signal for two cracks/slots (not covered with paint) with the same width (~0.200 mm) but different depths (0.5 mm and 0.75 mm) at a frequency of 11.3 GHz.

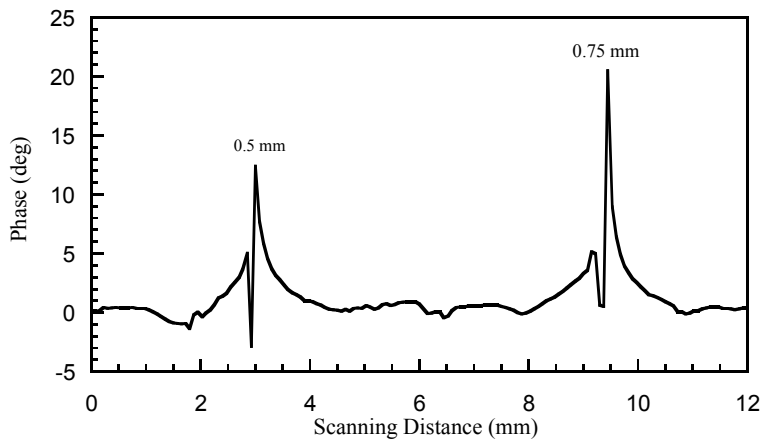

Figure 36a. Crack characteristic signal at 11.3 GHz for a slot with a width of ~0.200 mm and with different depths, coax inner radius of 0.5 mm and outer radius of 1.5 mm.

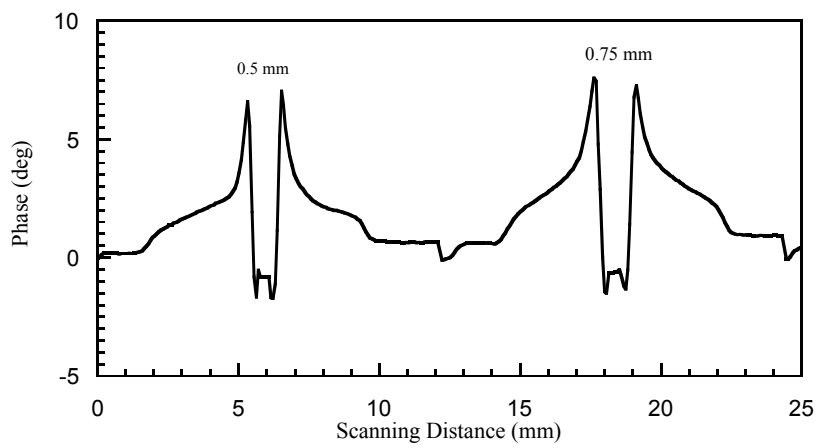

Figure 36b. Crack characteristic signal at 11.3 GHz for a slot with a width of ~0.200 mm and with different depths, coax inner radius of 1.0 mm and outer radius of 4.0 mm.

To show the potential of this method for detecting tight surface cracks, a fatigue specimen with a 3 μm-wide crack was inspected using the smaller coaxial probe (0.5 mm inner radius and 1.5 mm outer radius) and at a frequency of 11.3 GHz. Figure 37 show the results of the scan; as can be seen the technique is clearly capable of detecting very tight fatigue cracks.

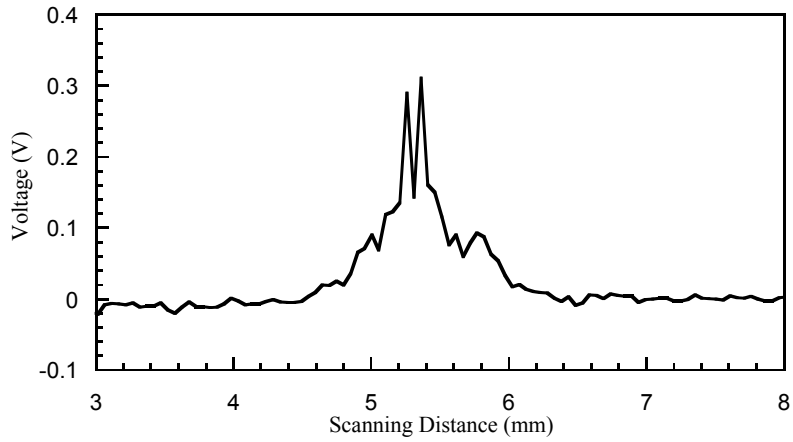

Figure 37. Crack characteristic signal for a fatigue crack with a width of ~3 μm and at a frequency of 11.3 GHz.

The primary goal of this investigation was to detect fatigue cracks that were covered by paint, therefore, to simulate varying paint thickness, sheets of 0.025 mm thick tissue paper was used to cover cracks that were subsequently scanned. Figures 38 (a) and 38 (b) show the results for a crack/slot with a width of 0.25 mm and a depth of 1.0 mm at a frequency of 10.5 GHz for four different tissue paper thicknesses. It is obvious that as the coating thickness increases, the dynamic range of the detected signal decreases. Another point to note is that there is now only peak in the crack characteristic signal while there are two peaks for the case when there is no coating. This is due to the fact that the crack no longer directly interacts with the inner conductor of the coaxial probe and consequently, the two peaks that were seen previously are combined into one.

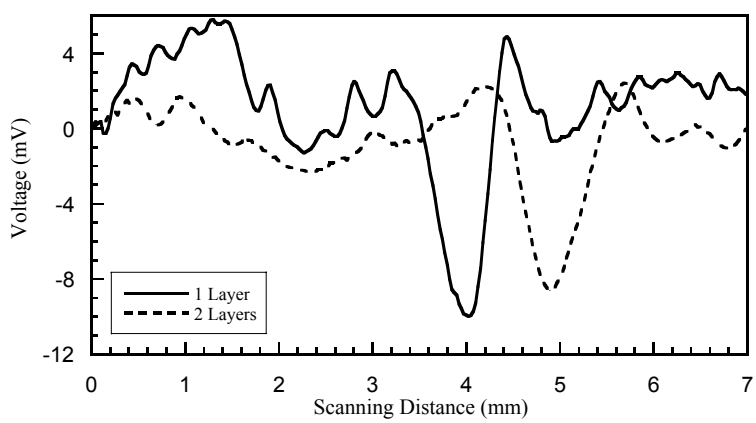

Figure 38a. Crack characteristic signal for covered crack with one and two layers of tissue paper.

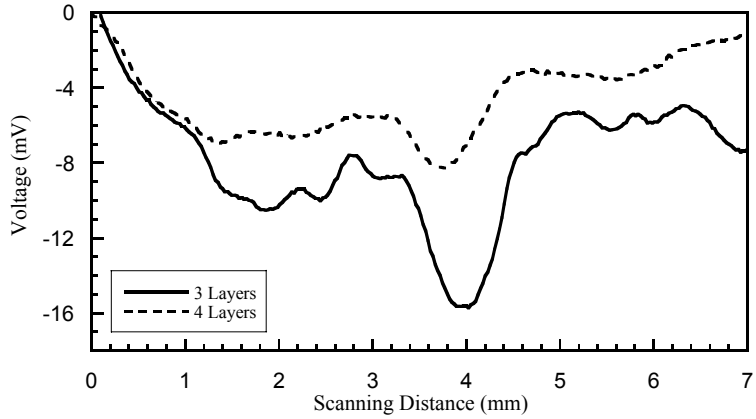

Figure 38b. Crack characteristic signal for covered crack with three and four layers of tissue paper.

Figure 39 shows the effects of frequency and incident power in covered crack detection. At a frequency of 11.37 GHz the detected dynamic range is larger than that at a frequency of 10.33 GHz. Measurements show that the optimal frequency for detection depends on the combination of the different crack sizes and the coax size. Regarding incident power, if the power is too low the electric field may not be able to penetrate through the paint and reflect back to the coax aperture. In this case the crack will not be seen. Examining the signals at 11.37 GHz and different power input (dB) in Figure 39, it can be seen that the dynamic range increases with increasing incident power.

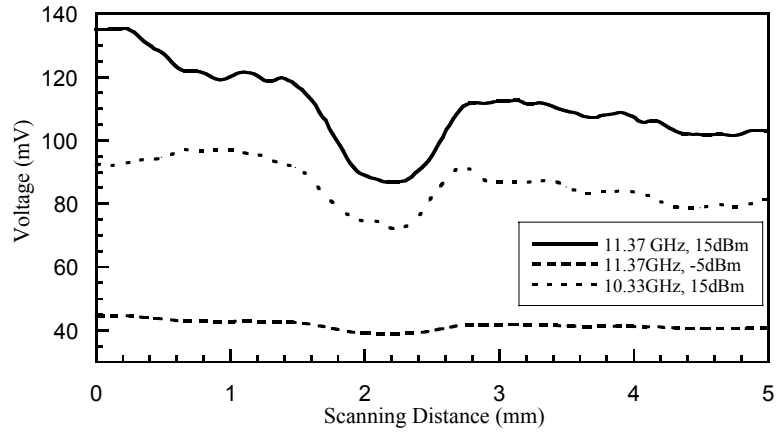

Figure 39. Influence of frequency and incident power on covered crack detection for a slot with a width of 0.15 mm and a depth of 0.75 mm and coating (tape) thickness of 0.11 mm.

When a rectangular waveguide, operating in its dominant mode (TE_{10}), is terminated with a metal plate, it is effectively short-circuited and there is no electric field component along the direction of the broad side of the rectangular waveguide. However, if there is a crack in the metal plate, the crack changes the reflection properties of the plate and hence the waveguide is no longer short-

circuited, the electric field is disturbed, and higher-order modes are generated. This causes an electric field component in the direction along the broad side of the waveguide. By detecting this electric field, the presence of a crack can be indicated. This is a very sensitive method for detecting cracks. Such a probe was used to examine the potential of this method for detecting covered cracks as well.

Similar to the coaxial probe approach, measurements were conducted by moving the aperture of the open-ended rectangular probe along the surface under inspection. The recorded voltage is related to the power associated with the presence of high-order modes as a result of the presence of a crack in a metal plate. Measurements were conducted in the Ka-band frequency range (26.5 - 40 GHz) that was previously determined to be a suitable frequency range for this purpose [2].

For the open-ended rectangular waveguide crack characteristic signal, there are issues concerning the flange edge effect. When there is no dielectric layer between the waveguide and the metal plate, we expect two peaks as the two edges of the waveguide aperture come across the crack. However, when there is a dielectric layer between the waveguide and the metal plate, there may exist an electric field propagating in the dielectric layer, and the detected signal changes four times as the two edges of the flange and two edges of the aperture scan across the crack [2, 12]. The relative amplitude of the multiple peaks depends on the operating frequency, dielectric property and thickness of the coating, and also the probe location.

Figure 40 shows the results when scanning a slot on a brass sample at a frequency of 31.5 GHz. Figure 40 (a) is for the case when the crack is uncovered. The airgap between the waveguide and the metal plate cause the multiple peaks (more than two). Figure 40 (b) and 40 (c) show the results from scanning the same crack under coating (clear tape) thickness of 0.05 mm and 0.15 mm. For all three cases shown in Figure 40, the signal level is low in the region where the crack is outside of the waveguide aperture. Theoretically if there is no coating there should be no signal detected and the signal-to-noise ratio is infinity. The high signal-to-noise level is the most prominent characteristic of the open-ended rectangular waveguide probe [2]. Also, the multiple peaks increase the probability of crack detection.

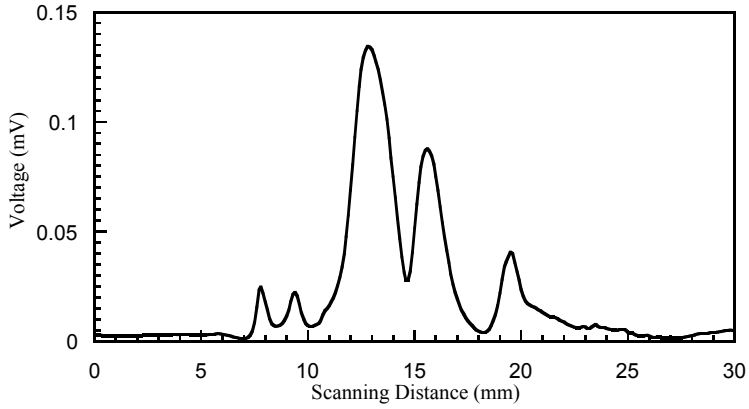

Figure 40a. Higher order mode signal generated by the open-ended rectangular waveguide probe for an exposed crack with a width of ~0.1 mm and a depth of 0.9 mm.

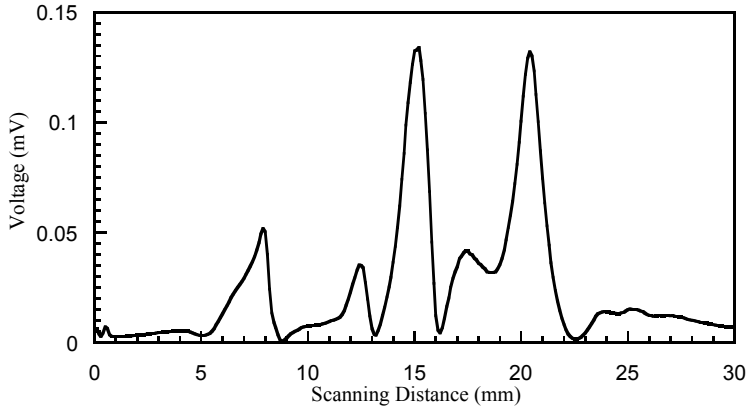

Figure 40b. Higher order mode signal generated by the open-ended rectangular waveguide probe for a covered crack with a coating thickness of 0.05 mm and crack width of ~0.1 mm and a depth of 0.9 mm.

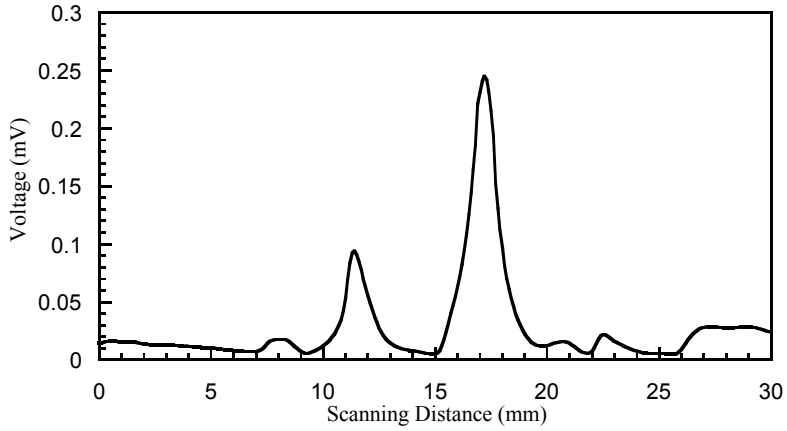

Figure 40c. Higher order mode signal generated by the open-ended rectangular waveguide probe for a covered crack with a coating thickness of 0.15 mm and crack width of ~0.1 mm and a depth of 0.9 mm.

Extensive sets of measurements over a wide range of cracks were conducted using coaxial and open-ended rectangular (higher order mode) waveguide probes. Both coated and uncoated fatigue cracks and slots were studied in this investigation. The results indicate that both probes have high potential for detecting cracks under coatings such as paint and primer. Each probe possesses its unique advantages and disadvantages. The coaxial probe was shown to easily be able to detect tight cracks under coatings of about 0.15 mm at relatively low microwave frequencies (X-band). The coaxial probe was also found to be less susceptible to edge effect issues. The open-ended rectangular (higher order mode) waveguide probe also showed the ability to detect similar cracks under like coatings, however, the issues of edge effects and small changes in the standoff distance seem to be more of a concern when using this probe.

Detection of corrosion

Three aluminum plates were prepared for the experimental investigation of detecting hidden corrosion using open-ended rectangular waveguide probes. One panel, used as the control sample, was free of corrosion. The other two panels (B and C) were halfway submerged in salt water in order to generate corrosion products (Figure 41). Both halves of the plate contained some corrosion products, however, the bottom halves of the plate contained pitting due to the presence of salt products, while the top half remained smooth. Excess salt was removed from the plates, and they were then sand blasted to remove the corrosion. Both the front and back panels of the plates had masks placed on them to retain areas of corrosion during sand blasting. The fronts of the panels were left with a strip of corrosion about 3 inches wide running down the center of the plate from top to bottom, and the backs of the panels were masked so that there was a square of corrosion on the pitted area. The plates were then primed and painted.

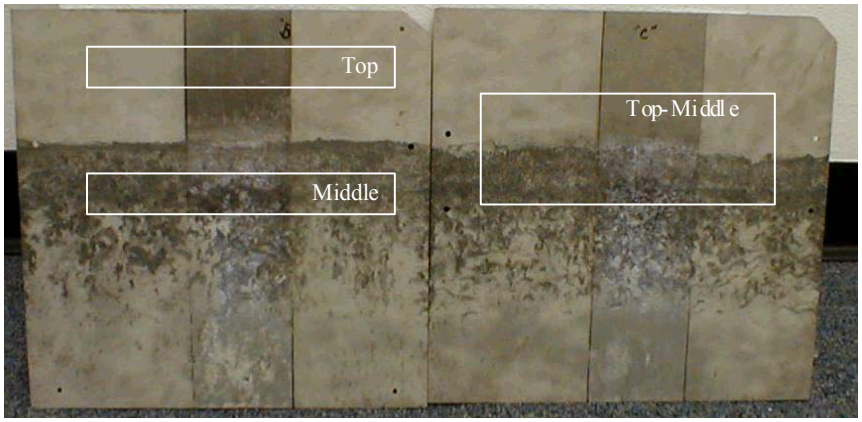

Figure 41. Sample plates C (left) and B (right) showing corrosion before being painted, with areas scanned highlighted.

The experimental investigation involved performing two-dimensional area scans with an open-ended waveguide probe. The areas scanned included strips along the top of the plate (where no pitting was present), strips along the middle of the plate (where pitting was present), strips along both the top and middle of the plate (where there contained areas with and without pitting). Scans of the entire plate were also performed. These scans were performed using different frequencies of operation, as well as adjusting the standoff distance of the waveguide probe [18].

Figure 42 shows an area scan of the top-middle strip of the front of panel B. The darker area of the image represents the corroded area in the panel. Pitting can also be seen in the lower half of the image. The frequency of operation was 24.1 GHz (K-band), and the waveguide probe was in contact with the surface (i.e. no standoff). Figure 43 shows the same scan as Figure 42, except the standoff distance was 5 mm in this case. Here, however, the lighter areas represent corrosion. Figure 44 shows an area scan of the top strip of the front of panel C. The frequency of operation was 24.1 GHz, and standoff distance was 5 mm. Again, the lighter area represents corrosion. Figure 45 shows an area scan of the middle strip of the front of panel C. Here, the darker area represents corrosion, and pitting can be easily seen. The frequency of operation was 33.5 GHz (K-band), and the standoff distance was 2 mm. Figure 46 shows an area scan of the top-middle strip of the front of panel C. The frequency of operation and standoff distance is the same as in Figure 45.

It was observed that as frequency of operation increased, the corroded area could be more easily distinguished from the non-corroded area. This observation matches the results from the theoretical analysis. Also, since the waveguide aperture is smaller at higher frequencies, pitting can be seen in greater detail as higher frequency bands are used.

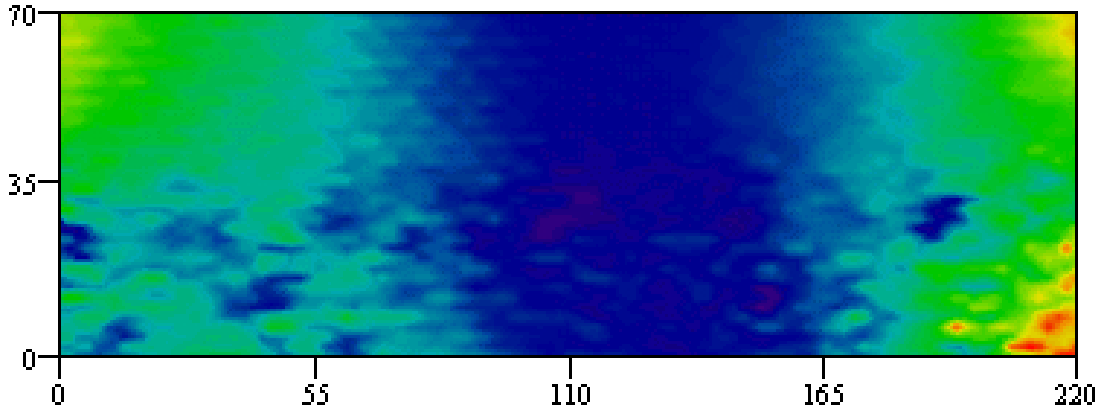

Figure 42. Image acquired using an open-ended rectangular waveguide probe of the top-middle strip of the front of panel B, at a frequency of 24.1 GHz and at a standoff distance of 0 mm (i.e. in contact). (Note: Dimensions are in mm).

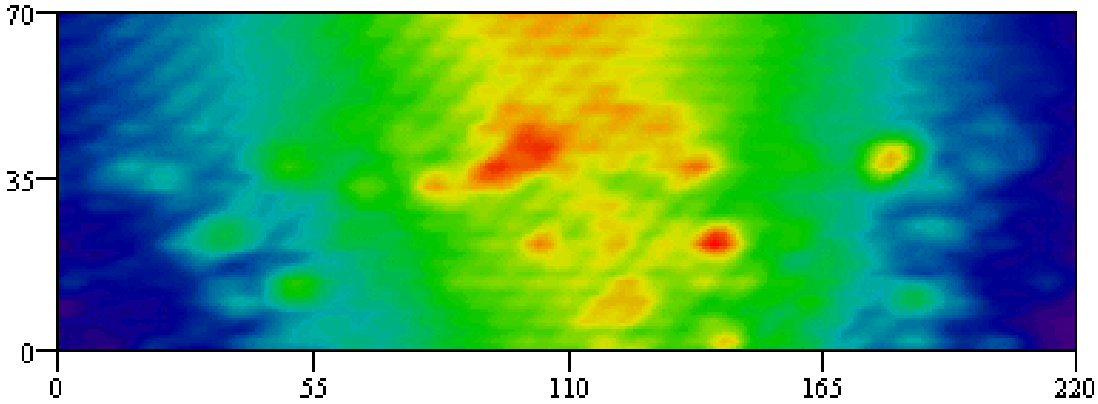

Figure 43. Image acquired using an open-ended rectangular waveguide probe of the top-middle strip of the front of panel B, at a frequency of 24.1 GHz and at a standoff distance of 5 mm. (Note: Dimensions are in mm).

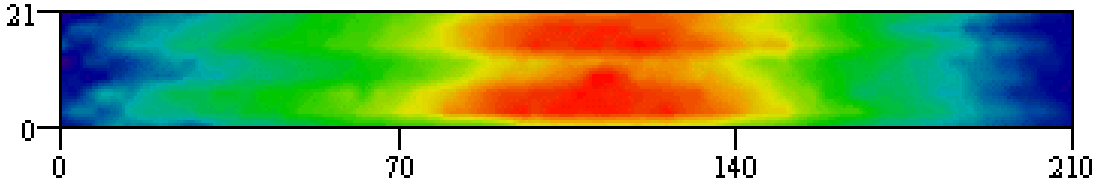

Figure 44. Image acquired using an open-ended rectangular waveguide probe of the top strip of the front of panel C, at a frequency of 24.1 GHz and at a standoff distance of 5 mm. (Note: Dimensions are in mm).

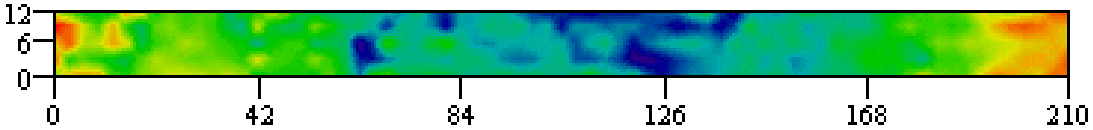

Figure 45. Image acquired using an open-ended rectangular waveguide probe of the middle strip of the front of panel C, at a frequency of 33.5 GHz and at a standoff distance of 2 mm. (Note: Dimensions are in mm).

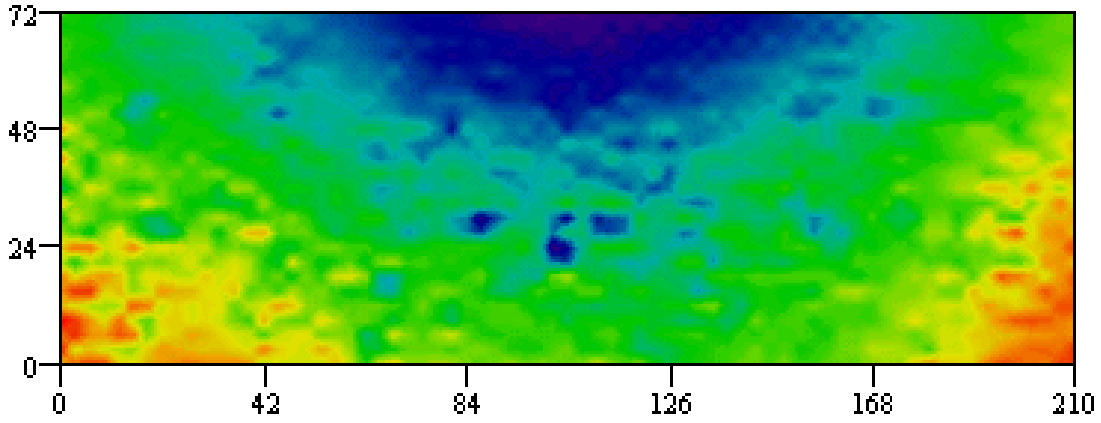

Figure 46. Image acquired using an open-ended rectangular waveguide probe of the top-middle strip of the front of panel C, at a frequency range of 33.5 GHz and at a standoff distance of 2 mm. (Note: Dimensions are in mm).

It was found that dielectric properties of aluminum oxide, paint and primer are very similar to each other. This is important since it is easier to detect corrosion under paint when the dielectric properties have a greater difference when compared to each other, as is the case with steel corrosion. Regardless, it was possible to detect corrosion in aluminum under a layer of paint and primer using near-field microwave nondestructive techniques with open-ended rectangular waveguide probes.

OTHER PROJECT ACCOMPLISHMENTS

This project, supported by the SERDP Program Office, has lead to the advancement of nondestructive evaluation technologies for the inspection of fatigue cracks and corrosion hidden under coatings. This work has resulted in the publication of eight papers, the submission of three reports (not including the current document), and the presentation of seven technical talks at national and international conferences. An application has been made by Imperium, Inc. and the Naval Air Warfare Center Aircraft Division (NAWC-AD) for the issuance of a patent based on the oblique angle beam real-time ultrasound imaging system. Imperium is also fabricating the first through transmission real-time ultrasound imaging system for Boeing/Vertol in Philadelphia as a direct consequence of this work. Finally, Thermal Wave Imaging, Inc. developed and demonstrated a field portable pulse thermography unit for the inspection of corrosion hidden under paint.

CONCLUSIONS

Three different innovative nondestructive evaluation technologies were developed and evaluated for the ability to detect fatigue cracks and corrosion hidden under paint. The three technologies included real-time ultrasound imaging, thermal imaging, and near-field microwave imaging. With each of these nondestructive inspection methods, subtasks were performed in order to optimize each methodology.

For the ultrasound imaging technique three different configurations of camera were developed by Imperium, Inc. in order to acquire an image of a sample in real-time: through transmission, reflection (pulse-echo) and oblique angle beam. All of the camera systems were designed to be portable and all demonstrated the ability to detect light corrosion and fatigue cracks under paint. Two major accomplishments results from this work: (1) the first commercial aerospace unit for through transmission real-time ultrasound imaging is being fabricated for Boeing/Vertol Philadelphia, and (2) application has been made for the issuance of a patent based on the oblique angle beam system.

The thermal imaging techniques pursued by Thermal Wave Imaging and Wayne State University were fairly successful in their ability to detect light corrosion and fatigue cracks under paint. Thermal Wave Imaging evaluated the use of inductive heating, laser diode heating and pulse heating (flash lamps) as means to produce the heat gradients necessary to obtain thermographic images of test samples. The inductive heating and laser diode heating methods were more effective at detecting fatigue cracks than hidden corrosion, although both techniques had relatively low sensitivity owing to the low thermal contrast generated by the heat sources. The pulse heating technique was found to be very useful for the detection of hidden corrosion and showed the most promise for transitioning into the field owing largely to the portability of system. The main shortcoming of the pulse thermography system was the inability of the system to consistently locate fatigue cracks owing to the low thermal contrast between the base metal and the crack. In contrast, the sonic thermography system developed by Wayne State University was very effective in locating fatigue cracks in samples. Studies still need to be performed to determine the capabilities of sonic thermography for the detection of hidden corrosion.

The results of the near-field microwave imaging investigation conducted by Colorado State University and Texas Research Institute showed that there exists a high potential for detecting corrosion in aluminum under a layer of paint and primer using open-ended rectangular waveguide probes. Colorado State University also successfully demonstrated the use of these probes and coaxial probes for locating cracks under coatings. Coaxial probes were found to be less susceptible to edge effect issues than the open-ended rectangular waveguide probes. While near-field microwave imaging techniques have demonstrated

proof-of-principle concepts, further work is necessary before these techniques would be viable for field use.

TRANSITION PLAN

In order to support the transitioning of the technologies within this project, tasking was placed with four field activities: NADEP Jacksonville (FL), NADEP North Island (CA), Warner-Robins ALC (GA), and the Marine Corps Maintenance Center Albany (GA). An inspection requirements survey presented in Appendix A was developed and was completed by the Marine Corps Maintenance Center. Based on input from the Maintenance Center the questionnaire was to be revised and then sent to the other field activities. The revision was never completed and as a consequence the other field activities never received the survey. Appendix B contains the responses to the questionnaire sent to the Marine Corps Maintenance Center. A brief summary of the responses obtained from the Marine Corps Maintenance Center follows below.

The Marine Corps Maintenance Center did not identify paint removal as a requirement for performing nondestructive inspection on any of their platforms with the exception of the Light Armored Vehicle (LAV) where paint removal is required. In general, paint removal is dictated by the Statement-of-Work and not nondestructive inspection requirements. The LAV is depainted and inspected as a matter of course owing to its history of substrate stress and failure. In addition, paint removal is not performed chemically; rather paint is removed by blasting with glass or plastic grit. It was stated that there are situations under the IROAN Program (Inspect, Repair, Only As Necessary) where coating removal would not be necessary if the depots had an NDE technology that could inspect through the coating. The primary use of such NDE technology would be for the inspection of corrosion and cracks in the LAV. In general, the Marine Corps Maintenance Center would welcome any NDE technology that can locate corrosion and cracks, result in improved safety to the inspectors (as opposed to potential radiation hazards), and would eliminate the requirement for retaining a Level III inspector.

Of the three innovative nondestructive technologies developed and evaluated during the course of the SERDP program, the real-time ultrasound imaging and the pulse thermography system show the most promise for transitioning to the field. The through transmission approach to real-time ultrasound imaging has received considerable attention from the aerospace industry, in fact, Boeing/Vertol has accepted delivery of a through transmission unit to test composite components on the production line. The pulse thermography system is transitioning into the field because of successful demonstration of the abilities of the system to the aerospace community. NADEP Cherry Point NC has an older pulse thermography system that is currently used for limited applications. The system developed under the SERDP program will allow for an expansion of

these applications owing to the greater sensitivity of the new system as well as to its increased portability.

Sonic thermography has solicited a great deal of interest from the nondestructive evaluation community. Laboratory trials using actual aerospace components have been successful for the most part. Transitioning into the field, however, awaits the successful demonstration of a probability of detection determination in the case of a major application such as turbine engine components. Funding is being pursued in order to implement the transition of the technology.

The near-field microwave imaging program was capable of demonstrating proof-of-principle for using microwave techniques to inspect for fatigue cracks and corrosion hidden under paint. Additional work needs to be performed before the current systems (open-ended coaxial and open-ended rectangular waveguide probes) could be viable for field inspections.

REFERENCES

1. Zoughi, R., S. Ganchev, C. Huber, E. Ranu and R. Runser, "A Novel Microwave Method for Filled and Covered Surface Crack Detection in Steel Bridges Including Crack Tip Identification," Final (Fourth Quarterly) Report, Federal Highway Administration (FHWA), Grant no. DTFH61-94-X-00023, p. 187, September 1995.
2. Qaddoumi, N., E. Ranu, R. Mirshahi, P. Stepanek, V. Otashevich, C. Huber and R. Zoughi, "Development of Equipment for and Quantitative Analysis of Microwave Detection and Evaluation of Fatigue Induced Surface Cracks in Steel," Final Report, Federal Highway Administration (FHWA), Grant no. DTFH61-94-X-00023, p. 519, January 1998.
3. Yeh, C., E. Ranu and R. Zoughi, "A Novel Microwave Method for Surface Crack Detection Using Higher Order Waveguide Modes," *Materials Evaluation*, vol. 52, no. 6, pp. 676-681, June 1994.
4. Huber, C. and R. Zoughi, "Higher Order Modes as Indicators of Surface Cracks Under Stratified Dielectric Coatings Using an Open-Ended Waveguide," *Proceedings of the Review of Progress in Quantitative NDE*, vol. 14A, pp. 637-642, 1995.
5. Yeh, C. and R. Zoughi, "A Novel Microwave Method for Detection of Long Surface Cracks in Metals," *IEEE Transactions on Instrumentation and Measurement*, vol. 43, no. 5, pp. 719-725, October 1994.
6. Yeh, C. and R. Zoughi, "Microwave Detection of Finite Surface Cracks in Metals Using Rectangular Waveguide Sensors," *Research in Nondestructive Evaluation*, vol. 6, no. 1, pp. 35-55, 1994.
7. Yeh, C. and R. Zoughi, "Sizing Technique for Surface Cracks in Metals," *Materials Evaluation*, vol. 53, no. 4, pp. 496-501, April 1995.
8. Huber, C., S.I. Ganchev, R. Mirshahi, J. Easter and R. Zoughi, "Remote Detection of Surface Cracks/Slots Using Open-Ended Rectangular Waveguide Sensors: An Experimental Investigation," *Nondestructive Testing & Evaluation*, vol. 13, pp. 227-237, 1997.
9. Ganchev, S., R. Zoughi, C. Huber, R. Runser and E. Ranu, "Microwave Method for Locating Surface Cracks Tips in Metals," *Materials Evaluation*, vol. 54, no. 5, pp. 598-603, May 1996.
10. Huber, C., H. Abiri, S. Ganchev and R. Zoughi, "Analysis of the Crack Characteristic Signal Using a Generalized Scattering Matrix Representation," *IEEE Transactions on Microwave Theory and Techniques*, vol. 45, no. 4, pp. 477-484, April 1997.
11. Huber, C., H. Abiri, S. Ganchev and R. Zoughi, "Modeling of Surface Hairline Crack Detection in Metals Under Coatings Using Open-Ended Rectangular Waveguides," *IEEE Transactions of Microwave Theory and Techniques*, vol. 45, no. 11, pp. 2049-2057, November 1997.
12. Qaddoumi, N., E. Ranu, J.D. McColskey, R. Mirshahi and R. Zoughi, "Microwave Detection of Stress Induced Fatigue Cracks in Steel and Potential for Crack Opening Determination," *Research in Nondestructive Evaluation*, vol. 12, no. 2, pp. 87-103, 2000.

13. Wang, Y. and R. Zoughi, “Interaction of Surface Cracks in Metals with Open-Ended Coaxial Probes at Microwave Frequencies,” *Materials Evaluation*, vol. 58, no. 10, November 2000.
14. Zoughi, R., K. Hayes and S. Ganchev, “Microwave Detection of Hairline Surface-Breaking Cracks in Metals Using Open-Ended coaxial Sensors: Preliminary Results,“ *Proceedings of SPIE Symposium, Nondestructive Evaluation Techniques for Aging Infrastructure & Manufacturing Conferences*, vol. 2945, pp. 444-450, Scottsdale, AZ, December 2-5, 1996.
15. R. Zoughi, C. Huber, J. Easter and K. Hayes, “Microwave Detection of Surface Cracks in Metals Under Dielectric Coatings Using Open-Ended Coaxial Sensors: Preliminary Results,” Special Topics Proceedings of *Nondestructive Evaluation of Infrastructure*, edited by H. Reis and B. Djordjevic, 1997.
16. Qaddoumi, N., L. Handjojo, T. Bigelow, J. Easter, A. Bray and R. Zoughi, “Microwave Corrosion Detection Using Open-Ended Rectangular Waveguide Sensors,” *Materials Evaluation*, vol. 58, no. 2, pp. 178-184, February 2000.
17. Qaddoumi, N., A. Shroyer and R. Zoughi, “Microwave Detection of Rust Under Paint and Composite Laminates,” *Research in Nondestructive Evaluation*, vol. 9, no. 4, pp. 201-212, 1997.
18. Wang, N., D. Hughes, K. Donnell, T. Case and R. Zoughi, “Feasibility Study of Corrosion Detection Under Paint in Aluminum Panels,” Final Report, Texas Research Institute at Austin (TRI-Austin), July 2000.

APPENDIX A

The following is a survey that was written in order to support the transitioning of the nondestructive inspection methods developed and evaluated under the SERDP Program. The survey was sent to the Marine Corps Maintenance Center Albany (GA) and responses to this questionnaire appear in Appendix B. Based on input from the Maintenance Center the questionnaire was to be revised and then sent to the three other field activities: NADEP Jacksonville (FL), NADEP North Island (CA) and Warner-Robins ALC (GA). The revision was never completed and as a consequence the other field activities never received the survey.

NSWC Carderock / SERDP PP-1134
Crack and Corrosion Inspection Needs Survey for Field Activities

The following list of questions was developed as a basis for gathering information on inspection requirements and technology implementation constraints. While an effort was made to develop a list of comprehensive questions, the list is not necessarily all-inclusive. If there is additional information that you think may be useful, please include it along with your other responses.

1. Identify the types of aircraft or vehicles that are currently worked on at your facility.
2. What types of NDE inspections are performed on each of these vehicle types?

- What is the purpose for conducting the inspection? When is the inspection conducted?
- What is the substrate material?
- What is the geometry of the inspection region?
- Is any surface preparation required?
- If there are corrosion issues, identify the corrosion type, etc.
- If there are crack issues, identify the type, length, orientation or geometry.

3. Identify current inspection requirements that necessitate the removal of coatings. (ID inspection procedures and describe stripping requirements, if possible.)

- Could coating removal be avoided if the NDE inspection technology could inspect through the coating?

4. For instances where coatings are removed:
   - What platforms/vehicles & how many are stripped per year?
   - What chemicals are used to strip? How many gallons per vehicle?
   - How much waste is generated? What is the disposal cost?

- What are the outyear projections for these processes?

5. Identify an individual cognizant for pollution issues in your local environmental quality office and provide their contact information (phone, fax, email)
6. Identify the limits of current techniques and the resolution that will be required if a new inspection technology was to be introduced into service.
7. Identify constraints on new NDE system implementation:

- Acquisition cost
- Portability
- Size & dimensions
- Weight
- Power
- Safety
- Other

APPENDIX B

The following are responses to a questionnaire designed to assist the investigators of the SERDP Program with transition plans for implementing the technologies developed and evaluated during the course of this program. The responses come from the Marine Corps Maintenance Center Albany (GA).

NSWC Carderock / SERDP PP-1134

Crack and Corrosion Inspection Needs Survey for Field Activities

The following list of questions was developed as a basis for gathering information on inspection requirements and technology implementation constraints. While an effort was made to develop a list of comprehensive questions, the list is not necessarily all-inclusive. If there is additional information that you think may be useful, please include it along with your other responses.

1. Identify the types of aircraft or vehicles that are currently worked on at your facility.
   Please refer to Table 1.
2. What types of NDE inspections are performed on each of these vehicle types?
   - What is the purpose for conducting the inspection? When is the inspection conducted?
   - What is the substrate material?
   - What is the geometry of the inspection region?
   - Is any surface preparation required?
   - If there are corrosion issues, identify the corrosion type, etc.
   - If there are crack issues, identify the type, length, orientation or geometry.

   Please refer to Table 1.
3. Identify current inspection requirements that necessitate the removal of coatings (ID inspection procedures and describe stripping requirements, if possible).
   - Could coating removal be avoided in the NDE inspection if technology could inspect through the coating?

   Vehicle coating removal for the normal maintenance cycle is primarily driven by the Statements-Of-Work (SOWs), which require the removal of coatings. There are situations under the IROAN Program (Inspect, Repair, Only As Necessary) that coating removal would not be necessary if the depots had NDE technology that could inspect through the coating.
4. For instances where coatings are removed:
   - What platforms/vehicles & how many stripped per year?

The primary focus of a new NDE system would be on the LAV. The five-year average would be in the 70-80 vehicles per year range. Other weapons platforms are also involved in this process on an "as required" basis, but virtually every LAV is inspected due to vehicle history.

- What chemicals are used to strip? How many gallons per vehicle?

Neither USMC maintenance center is currently using chemicals to strip paint. The preferred method is blasting.

- How much waste is generated? What is the disposal cost?

Maintenance Center Albany generated 36,404 lbs of plastic blast grit in FY98 and 25,179 lbs. of glass blast grit. Maintenance Center Barstow data was not forthcoming but it is estimated that they generated approximately 15-20% more because they paint more vehicles.

- What are out year projections for these processes?

The USMC maintenance centers do not anticipate utilizing any stripping method in out years that would involve chemicals to any great degree. It is possible that some form of high pressure water stripping could be utilized but not likely in the near future. The Applied Research Lab of Penn State University has a current research project underway funded by the ManTech Program to identify a commercially available, environmentally benign chemical paint stripper or process. Implementation would be dependent upon successful testing. The chemical paint stripping or alternative process would likely be used as pre-stripping paint softener to reduce our use of blast media.

5. Identify an individual cognizant for pollution issues in your local environmental quality office and provide their contact information (phone, fax, e-mail).
   Lamaar Petties
   Phone: (229) 639-6826
   Fax: (229) 639-
   E-Mail: pettiesl@matcom.usmc.mil
6. Identify the limits of current techniques and the resolution that will be required if a new inspection technology was to be introduced into service.
   Current technology presents the following limitations:
   THROUGHPUT - *The current process is labor intensive and as a result can create a vehicle throughput problem. It requires an intensive set-up and repositioning effort and the time required to "shoot" a vehicle is too long. Any new technology needs to improve on this problem.*
   EFFICIENCY *– The cost of retaining a Level 3 inspector, film storage and handling, and manpower requirements are examples of our current technology's inefficiency. When shooting a vehicle, "guards" are posted to prevent inadvertent entry and exposure to the NDE area. These guards are an unnecessary expense and their time and effort could be better utilized. The cost of handling and storing film is a serious financial burden and any new technology that could reduce or eliminate this requirement would be welcomed. MCA is currently considering retaining the services*

of a Level 3 inspector specifically for the requirements of NDE. New technology that would eliminate this requirement would also be welcomed.
***SAFETY** – The fact that MCA posts guards during NDE operations is pretty indicative of the safety hazards present. Obviously, one of the driving factors of new technology has been the potential reduction or elimination of these hazards. The implementation of any new technology would almost certainly need to have the promise of improved safety issues.*
***ACCURACY** - The USMC is facing some pretty serious cracking issues with the LAV armor plate. Putting troops in the field with the prospect of vehicle armor that has the potential to have unidentified cracks or suffering from reduced ballistic characteristics is a scenario that needs to be addressed.*

7. Identify constraints on new NDE system implementation:
    - Acquisition cost
    - Portability
    - Size and dimensions
    - Weight
    - Power
    - Safety
    - Other

    These constraints are discussed in Table 2.

Table 1. Vehicle Types and Inspection Data

VEHICLES	SUBSTRATE	CORROSION ISSUES	CORROSION TYPE	SURFACE PREP REQ.	CRACK ISSUES	ID TYPE, LENGTH, ORIENTATION, GEOMETRY
AAV	5083 Aluminum 1020 Steel	Yes	Primarily Stage 1-2, incidents of Stage 3 on steel components[1]	Paint is not removed for NDE purposes[3]	No	Not an issue
LAV	00461 High Armor steel 1020 steel	Yes	Primarily Stage 1-2, incidents of Stage 3 on steel components[1]	Yes – paint must be removed	Yes	Figures identifying primary areas and length of cracks can be provided as an attachment if required[2].
M88	Primarily 1020 steel	Yes	Primarily Stage 1-2, incidents of Stage 3 on steel components[1]	Paint is not removed for NDE purposes[3]	No	Not an issue
HMMWV	Primarily 1020 steel	Yes	Primarily Stage 1-2, incidents of Stage 3 on steel components[1]	Paint is not removed for NDE purposes[3]	No	Not an issue
M-923 5-Ton Cargo Truck	Primarily 1020 steel	Yes	Primarily Stage 1-2, incidents of Stage 3 on steel components[1]	Paint is not removed for NDE purposes[3]	No	Not an issue
M-105A2 Cargo Trailer	Primarily 1020 steel	Yes	Primarily Stage 1-2, incidents of Stage 3 on steel components[1]	Paint is not removed for NDE purposes[3]	No	Not an issue
M1A1 Tank	High armor steel	Yes	Primarily Stage 1-2, incidents of Stage 3 on steel components[1]	Paint is not removed for NDE purposes[3]	No	Not an issue
MK14 Trailer, Container	Primarily 1020 steel	Yes	Primarily Stage 1-2, incidents of Stage 3 on steel components[1]	Paint is not removed for NDE purposes[3]	No	Not an issue

NOTES

1. There have been incidents of Stage 3 – 4 corrosion in certain areas: battery boxes, inaccessible areas of the frames, door jambs, etc.
2. Historical records have been kept going back several years on each LAV that has passed through the Albany Maintenance Center. These records include a graphical reproduction on the location, length, date, vehicle #, geometry, and disposition. The records are very detailed and have been retained in several notebooks.
3. Vehicle depainting is generally driven by the Statement-of-Work (SOW) not NDE requirements. Vehicles with a history of substrate stress and failure (LAV) are depainted and inspected as a matter of course.

Table 2. System Constraints

Acquisition Cost	Portability	Size/ Dimensions	Weight	Power	Safety	Other
Don't know that there is a ceiling on this issue. Funding would be dependent on the functionality, flexibility, and safety of a new system. The costs of operating and maintaining current system is extremely expensive but an ROI assessment would have to be conducted.	Current system equipment has little or no portability. Portability would be a desired characteristic of new system but not required.	Current system has a dedicated facility. Size is not a big issue but new system should be able to utilize current facility without any major construction or refacilitization.	We are looking for something more portable and smaller than our current system. A new system that meets these desires would, by nature, be lighter.	Power should be commensurate with current requirements. The planned site survey would probably resolve this issue. We do not anticipate the power needs of any new technology being greater than our current process.	Current system has some serious safety issues and is one of the prime reasons that a new system is being evaluated. Any new system must be dramatically safer!	We are currently required to retain the services of a level III inspector. We are also handling and storing film. A reduction of these requirements would also be desirable.

APPENDIX C

The following reports, presentations, and other associated professional works were produced during the course of the SERDP Project. Where available the reports appear in full.

Papers

Han, X., L.D. Favro, and R.L. Thomas, "Recent Developments in Thermosonic Crack Detection," *Review of Progress in Quantitative Nondestructive Evaluation*, Vol. 21, (to be published).

Ouyang, Z., L.D. Favro, R.L. Thomas, and X. Han, "Theoretical Modeling of Thermosonic Imaging of Cracks," *Review of Progress in Quantitative Nondestructive Evaluation*, Vol. 21, (to be published).

Perez, I. and X. Han, "Pulsed Thermographic Modeling," *Review of Progress in Quantitative Nondestructive Evaluation*, Vol. 21, (to be published).

Hughes, D., N. Wang, T. Case, K. Donnell, R. Zoughi, R. Austin, and M. Novack, "Microwave Nondestructive Detection of Corrosion Under Thin Paint and Primer in Aluminum Panels," *Subsurface Sensing Technologies and Applications*, Vol. 2, No. 4, pp. 435-451, October 2001.

Hughes, D., N. Wang, T. Case, K. Donnell, R. Zoughi, R. Austin, and M. Novack, "Detection of Corrosion in Aluminum Panels Under Paint and Primer," *Review of Progress in Quantitative Nondestructive Evaluation*, Vol. 20, edited by D.O. Thompson and D.E. Chimenti, 2001.

Wang, N., K. Donnell, M. Castle, R. Zoughi, and M. Novack, "Microwave Detection of Covered Surface Cracks in Metals," *Review of Progress in Quantitative Nondestructive Evaluation*, Vol. 20, edited by D.O. Thompson and D.E. Chimenti, 2001.

Davis, W.R. and B. Lasser, "Development of Real Time Ultrasonic Imaging," Proceedings of the 54th Meeting of the Machinery Failure Prevention Technology Society, 1-4 May 2000, Virginia Beach, Virginia.

Perez, I. and P. Kulowitch, "Thermography for Characterization of Corrosion Damage," Proceedings of the National Association of Corrosion Engineers (NACE) Expo 2000, 27-30 March 2000, Orlando, Florida.

Reports

Novack, M. and I. Perez, "Development of Innovative Nondestructive Evaluation Technologies for the Inspection of Cracking and Corrosion Under Coatings, SERDP PP-1134," FY00 Annual Report, March 2001.

Wang, N., K. Donnell, M. Castle and R. Zoughi, "Microwave Detection of Cracks in Painted Metallic Substrates," Final Report submitted to Michele Novack, October 2000.

Novack, M. and I. Perez, "Development of Innovative Nondestructive Evaluation Technologies for the Inspection of Cracking and Corrosion Under Coatings, SERDP PP-1134," FY99 Annual Report, March 2000.

Professional Presentations

Favro, Lawrence D. (Wayne State University), "Recent Developments in Thermosonic Crack Detection," 28th Annual Review of Progress in Quantitative Nondestructive Evaluation, Brunswick, Maine, 29 July - 3 August 2001.

Perez, Ignacio (Naval Air Warfare Center Aircraft Division), "Pulsed Thermographic Modeling," 28th Annual Review of Progress in Quantitative Nondestructive Evaluation, Brunswick, Maine, 29 July - 3 August 2001.

Ouyang, Zhong (Wayne State University), "Theoretical Modeling of Thermosonic Imaging of Cracks," 28th Annual Review of Progress in Quantitative Nondestructive Evaluation, Brunswick, Maine, 29 July - 3 August 2001.

Shepard, Steve (Thermal Wave Imaging, Inc.), "Thermographic Nondestructive Inspection of Metallic Aerospace Structures," 49th Annual Meeting of the Defense Working Group on Nondestructive Testing, hosted by the AF NDI Program Office and Keesler AFB, Biloxi, MS, 30 October-2 November 2000.

Chaudry, Brian (Thermal Wave Imaging, Inc.), "Application of Pulsed Thermography to Maintenance and Repair Inspections," Air Transport Association's 44th Annual Nondestructive Testing Forum, San Francisco, CA, 25-28 September 2000.

Wang, N. (Colorado State University), "Microwave Detection of Covered Surface Cracks in Metals," 27th Annual Review of Progress in Quantitative Nondestructive Evaluation, Ames, Iowa, 16-21 July 2000.

Hughes, D. (Colorado State University), "Detection of Corrosion in Aluminum Panels Under Paint and Primer," 27th Annual Review of Progress in Quantitative Nondestructive Evaluation, Ames, Iowa, 16-21 July 2000.

Conference Sessions

4th International Aircraft Corrosion Workshop, hosted by Naval Air Warfare Center Aviation Division, Solomons Island, MD, 22-25 August 2000.

- Dr. Perez chaired the session on Advanced Systems for Corrosion Detection and Monitoring Technologies

Patents

An application has been made for the issuance of a patent based on the oblique angle beam real-time ultrasound imaging system.